NASA-CR-204572

THE LOCAL Lyα FOREST: ASSOCIATION OF CLOUDS WITH SUPERCLUSTERS AND VOIDS[1,2]

John T. Stocke, J. Michael Shull,[3] and Steve Penton

Center for Astrophysics and Space Astronomy, University of Colorado, Boulder, CO 80309

030285

Megan Donahue

Space Telescope Science Institute, 3700 San Martin Drive, Baltimore, MD 21218

AND

Chris Carilli[4]

Sterrewacht Leiden, Postbus 9513 2300 RA Leiden, Netherlands

Received 1994 December 1; accepted 1995 April 3

ABSTRACT

The Goddard High Resolution Spectrograph aboard the *Hubble Space Telescope* was used with the G160M grating to obtain high-resolution (0.2 Å) spectra of three very bright active galactic nuclei located behind voids in the nearby distribution of bright galaxies (i.e., CfA and Arecibo redshift survey regions). A total of eight definite ($\geq 4\ \sigma$) Lyα absorption lines were discovered ranging in equivalent width from 26 to 240 mÅ at Galactocentric velocities 1740–7740 km s^{-1}. Of these eight systems, we locate seven in supercluster structures and one, in the sight line of Mrk 501 at 7740 km s^{-1}, in a void. In addition, one of two tentative (3–4 σ) Lyα absorption lines are found in voids. Thus, the voids are not entirely devoid of matter, and not all Lyα clouds are associated with galaxies. Also, since the path lengths through voids and superclusters probed by our observations thus far are nearly equal, there is some statistical evidence that the Lyα clouds avoid the voids. The nearest galaxy neighbors to these absorbing clouds are 0.45–5.9 Mpc away, too far to be physically associated by most models. The lower equivalent width absorption lines ($W_\lambda \leq 100$ mÅ) are consistent with random locations with respect to galaxies and may be truly intergalactic, similar to the bulk of the Lyα forest seen at high z. These results on local Lyα clouds are in full agreement with those found by Morris et al. (1993) for the 3C 273 sight line but are different from the results for higher equivalent width systems where closer cloud-galaxy associations were found by Lanzetta et al. (1994).

Pencil-beam optical and 21 cm radio line observations of the area of sky surrounding Mrk 501 fail to find faint galaxies near the velocities of the Lyα clouds in that sight line. Specifically, for the "void absorption" system at 7740 km s^{-1}, we find no galaxy at comparable redshift to the absorber within 100 h_{75}^{-1} kpc ($H_0 = 75\ h_{75}$ km s^{-1} Mpc^{-1}) with an absolute magnitude of $B \lesssim -16$ and no object with H I mass $\geq 7 \times 10^8\ h_{75}^{-2}\ M_\odot$ within 500 h_{75}^{-1} kpc. Thus, neither a faint optical galaxy nor a gas-rich, optically dim or low surface brightness galaxy is present close to this absorber.

Subject headings: large-scale structure of universe — quasars: absorption lines — intergalactic medium

1. INTRODUCTION

The discovery and delineation of cosmic "voids" in the spatial distribution of galaxies has been one of the more interesting aspects of extragalactic astronomy in recent years. How were these voids created? Is gravitational clustering of matter (light and dark) plus the biasing of light with respect to dark matter sufficient to produce voids of the size observed in the local universe, or are other more exotic mechanisms required: shock-wave–induced galaxy formation (Ostriker & Cowie 1981) or spacetime "textures" (Turok & Spergel 1990)? Failure to detect even low-mass galaxies in voids (Szomoru et al. 1994; Weinberg et al. 1991; Salzer et al. 1988) and the realization that the sizes of voids presently detected by galaxy surveys may be limited by the sizes of the surveys themselves have exacerbated these concerns. It is still uncertain whether the voids can be accounted for by standard gravitational physics and clustering models such as the cold or mixed dark matter theories with reasonable amounts of biasing of light versus dark matter (e.g., Frenk et al. 1990).

However, at higher redshifts ($z > 1.6$) systematic studies of the "forest" of hydrogen clouds detected by Lyα absorption lines in the spectra of distant QSOs find that these clouds do not exhibit the clustering in velocity expected for galaxies (e.g., Rauch et al. 1993) and so do not clearly show evidence for voids either (although see Dobrzycki & Bechtold 1991). That the Lyα forest clouds are a distinct population of objects from galaxies, perhaps a more "primeval" population of objects more evenly distributed in space, is one of the exciting possibilities that has driven the dedication of substantial amounts of large-aperture optical telescope time to their study. Certainly the expectations of the standard gravitational clustering models plus biasing of luminous matter compared to dark matter suggest that these lowest traceable mass clouds should be substantially less clustered than the more massive galaxies (Hamilton 1988; Bajtlik 1993; Mo & Morris 1994). Any of the standard clustering models would predict that some Lyα

clouds should be found in galaxy voids; indeed, the absence of clustering at high z for these clouds strongly suggests this possibility. But at $z > 1.6$ the distribution of galaxies is unknown, so that even the presence or absence of voids cannot be ascertained definitively at those redshifts.

Recent *Hubble Space Telescope* (*HST*) observations of the bright QSO 3C 273 made with the Faint Object Spectrograph (FOS; Bahcall et al. 1991) and the Goddard High Resolution Spectrograph (GHRS; Morris et al. 1991) detected numerous Lyα absorption lines at low z ($z < 0.16$). The detection of substantial numbers of these clouds was unexpected based upon a simple power-law extrapolation of dN/dz with z observed at higher redshifts. Whether pressure-confined models (Sargent et al. 1980; Ostriker & Ikeuchi 1983) could reproduce their numbers is still debatable given uncertainties about the magnitude and evolutionary rate of intergalactic medium (IGM) pressure and ionizing radiation field (Williger & Babul 1992; Charlton, Salpeter, & Hogan 1993). If these clouds are gravitationally confined by dark matter "minihalos" (Rees 1986, 1988; Bond, Szalay, & Silk 1988; Mo & Morris 1994), their numbers and clustering properties offer the possibility of studying the gravitational clustering of very low mass gas clouds, which could set additional constraints on the clustering theories. Specifically, studies of the local Lyα forest can directly test the potential association of Lyα clouds with galaxy voids as well as their clustering properties with respect to galaxies and to each other. While the Lyα detections in the *HST* spectra of 3C 273 are indeed local, in a sense they are not local enough to address their association with galaxy voids directly. Nearby large-angle galaxy redshift surveys (CfA survey, Huchra et al. 1990; Arecibo survey, Haynes & Giovanelli 1989), which are our primary data sets for defining the number, size, and structure of the voids, extend to only $z \sim 0.03$.[5] Furthermore, the Lyα clouds detected in the FOS 1 Å resolution spectra of other bright QSOs by the *HST* "Key Project" Team (Bahcall et al. 1993) or by other observers are almost all at much higher redshifts ($z \geq 0.2$) than even the 3C 273 Lyα clouds. The *HST* spectra of 3C 273 contained seven absorption lines with $z < 0.03$: three associated with the Local Supercluster (southern extension of the Virgo Cluster) and four evidently associated with the "Great Wall" (de Lapparent, Geller, & Huchra 1986) although the 3C 273 sight line is well south of the CfA redshift survey area. The absence of a large-angle galaxy redshift survey which includes the 3C 273 sight line means that the Lyα clouds detected by Morris et al. and Bahcall et al. cannot be directly related to any large-scale galaxy structures (other than the Virgo Cluster) like supercluster filaments or voids. In order to remedy this partially, Morris et al. (1993, hereafter M93) conducted a pencil-beam galaxy survey to $B = 19$ mag in a 1° area around 3C 273, so that some information relating galaxies to local Lyα clouds is available at present.

Here we present the initial results of a high spectral resolution study of very low redshift ($z \leq 0.03$) Lyα clouds in the direction of very bright active galactic nuclei (AGNs) which lie beyond regions well surveyed for galaxy redshifts. The purpose of our study is to detect Lyα absorption lines and to use the available redshift survey data to assist in determining the relationship (if any) between Lyα clouds and galaxies, supercluster structures, and cosmic voids. This study uses the *HST*/GHRS with the G160M grating to obtain ~ 50 km s^{-1} resolution spectra in the spectral range 1222–1258 Å ($cz = 1500$–$10,500$ km s^{-1}, or from the Local Supercluster to the "Great Wall"). The combination of the GHRS medium-resolution gratings and very bright background sources ($V \leq 14$ mag) allows very low detection thresholds for Lyα clouds of $W_\lambda \sim 50$ mÅ in exposure times of a few hours. Because of the very steep relationship observed between numbers of clouds and their column densities (e.g., Hunstead 1988; Carswell 1988) and the mean local Lyα cloud density of 1 cloud per 3500 km s^{-1} above $N(\text{H I}) = 10^{13}$ cm^{-2} (~ 50 mÅ) (Weymann 1993), this low equivalent width threshold allows the detection of a significant number of clouds (2–4 per sight line) despite the very limited wavelength coverage of these observations. This redshift range is the most valuable to probe for Lyα clouds because it is only at the lowest redshifts that the fainter galaxies and H I clouds can be detected optically and in the 21 cm emission line of hydrogen with radio interferometers. Thus, if low-luminosity or low surface brightness galaxies or even isolated H I clouds and H I tidal tails are responsible for some Lyα clouds, the very lowest redshift clouds can be scrutinized most carefully for these possibilities.

Up to the present, our project has obtained two completed GHRS + G160M (pre-COSTAR) observations of the bright Seyfert galaxy Markarian 335 ($V = 13.8$; $cz = 7500$ km s^{-1}) and the bright BL Lac object Markarian 501 ($V = 13.9$; $cz = 10,200$ km s^{-1}) and an incomplete observation of the quasar I Zw 1 ($V = 14.0$; $cz = 18,300$ km s^{-1}). Observations of a fourth target, Mrk 421 ($V = 13.5$, $cz = 9300$ km s^{-1}), will be obtained later (Shull, Stocke, & Penton 1995b). Based upon the galaxy redshift surveys in the areas between us and these targets, these three observations probe a path length equal to 11,800 km s^{-1} of supercluster and 11,400 km s^{-1} of void. Eight Lyα absorption lines are definitely detected by these observations; seven are in areas of galaxy superclusters, and one is in a cosmic void. In § 2 the observational details and analysis of these three spectra are presented. In § 3 the available galaxy survey data are used to characterize the locations of these clouds relative to galaxies. Section 4 describes additional efforts to find any galaxies associated with the Lyα cloud in the void toward Mrk 501. The discussion in § 5 summarizes our current understanding of the local Lyα forest and models of extended H I disks in light of these new observations. Section 6 includes a description of our future work planned with the *HST*/GHRS aimed at a better understanding of voids and the H I clouds detected by Lyα absorption lines.

2. OBSERVATIONS AND ANALYSIS

Basic information about the acquisition of the three G160M spectra is presented in Table 1. All spectra were obtained through the 2″ large science aperture (LSA) using the standard quarter-diode substepping pattern yielding pixels (quarter-diodes) of ~ 0.018 Å and an effective spectral resolution of ~ 7 pixels (30 km s^{-1}). The central wavelength was chosen to be 1240 Å, which allows detections of Lyα clouds at recessional velocities from 1500 to 10,500 km s^{-1} and covers the wavelengths of Galactic N V $\lambda\lambda 1238.821$, 1242.804 and S II $\lambda\lambda 1250.584$, 1253.811. The FP-split mode was utilized, so that the total exposure times shown in Table 1 were divided into sets of four individual integrations, between which the grating

---

[5] While the well-known Bootes void (Kirshner et al. 1981) has been shown to contain some galaxies (e.g., Szomoru 1994; Dey, Strauss, & Huchra 1990; Weistrop et al. 1992), it is more distant ($z \sim 0.05$) and less well defined than the voids in the CfA and Arecibo galaxy survey regions. Sensitive searches for dwarf and H I–emitting galaxies within these nearby survey regions (Salzer et al. 1988; Szomoru et al. 1994) find no field galaxies in the voids probed by the current observations.

TABLE 1

SUMMARY OF *HST*/GHRS SPECTRA OF BRIGHT AGNs BEHIND GALAXY VOIDS

Object	R.A.	Decl.	V	Velocity (km s^{-1})	Exposure Time (hr)	Approximate 4 σ Equivalent Width Limit (mÅ)
Mrk 335......	0034	+1955	13.8	7500	4.1	20
Mrk 501......	1652	+3950	13.9	10200	8.7	40
I Zw 1........	0050	+1225	14.0	18300	7.2	100

ᵃ Additional exposure time on I Zw 1 will be obtained during *HST* cycle 4; similar observations of Mrk 421 have been obtained during cycle 4 (Shull et al. 1995b).

was moved approximately 5 diodes. The spectra produced by the individual integrations were reduced using the STSDAS spectral reduction package within IRAF. Cross-correlations were performed on the individual FP-slit exposures of Mrk 335 using the Galactic S II absorption line in order to check for any possible wavelength drifts within the GHRS or target drifts within the LSA during the exposures; none were found. The individual split exposures of the other two targets were too noisy to perform a similar analysis, but there is no obvious indication of drifts. The overall continuum shape of these spectra was corrected for scattered geocoronal Lyα emission using a standard correction matrix supplied by the GHRS team. A seven-pixel Gaussian smoothing was used for final display and analysis. While higher count GHRS spectra seem to benefit from the application of a standard Lucy deconvolution algorithm using the line-spread function of the pre-COSTAR GHRS LSA (which is primarily Gaussian but with weak, extended wings; Gilliland et al. 1992; Brandt et al. 1993), we did not employ this routine with the current data (except to investigate widths of definite absorption lines; see below). This decision was based upon tests of the Lucy routines with these spectra, which revealed that the statistical significance of all ≥ 2.5 σ fluctuations was increased even if only one pass of the Lucy algorithm was employed. Since we suspect that some systematic noise might be present, the choice not to employ a deconvolution routine is conservative and results in a more secure line list.

The three final spectra are presented in Figure 1. The positions of all definite and tentative absorption lines are marked; the Galactic lines are indicated with a "G," the Lyα forest lines with an "L." The error spectrum based upon photon statistics alone is shown at the bottom of each plot.

The photon statistics were recomputed through each step, allowing an easy assessment of signal-to-noise ratio (S/N) as a function of wavelength. Because some photon-counting detector electronics produce "pattern noise," power spectra were computed for each summed spectrum; no evidence of pattern noise was found at any diode frequency for the Mrk 501 and I Zw 1 spectra. However, the higher quality Mrk 335 spectrum showed evidence for pattern noise with measurable power at all even-numbered diode spacings up to at least 8 and possibly to 16 diodes. The actual measured noise in line-free areas of the continuum exceeded the expected photon noise by $\sim 2^{1/2}$ in all three spectra. We have used these higher noise level estimates in computing absorption-line equivalent widths.

The wavelengths of the individual spectra were corrected slightly (≤ 75 km s^{-1}) for the position of the object in the LSA based upon the observed wavelength positions of the Galactic S II absorption features and the observed Galactic H I velocities in these directions. Because none of these sight lines contain significant high-velocity gas, the S II absorptions were

assumed to be at the local standard of rest (LSR). Based upon a scrutiny of the Heiles (1984) atlas of high-latitude H I, this assumption is generally accurate to ~ 5 km s^{-1}. We note the presence along the Mrk 501 sight line of the H I supershell designated GS 067 + 44 + 4 with H I velocities spanning $V_{LSR} = -8$ to $+16$ km s^{-1} (Heiles 1984), although the dominant H I emission at the position of Mrk 501 is at -4 km s^{-1}.

In order to determine the reality of the various absorption features, we assumed that all potential absorptions possessed single-Gaussian line profiles. The continuum was fitted using a quadratic polynomial in a 4–5 Å region surrounding each line, and noise levels were measured on either side of each potential line, thus assuming that no low-level absorption is present in those areas. A single-Gaussian profile was fitted simultaneously to each potential feature. This procedure always gave noise values slightly in excess of the formal noise computed from photon statistics as mentioned above and reduced χ^2 values of the fit to $\frac{1}{2}$ or less. Therefore, the errors in the equivalent widths of each line are dominated by the continuum placement uncertainty and thus by the actual noise in the continuum. We have verified this for a few individual lines by direct experiment.

All ≥ 4 σ lines are considered definite, and 3–4 σ lines "tentative". The reality of all ≥ 4 σ absorption lines was verified by dividing the summed exposures into quarters, both linear in time and by diode substep. The four very strong (≥ 8 σ) lines were detected in all four quarters of the data; the five 4–7 σ lines were detected in most of the quarters, and no quarter of the data dominated the detection of any of these lines.

Each detected line is listed in Table 2 with its particulars. The uncertainty in the equivalent widths can be determined directly from the significance level. The individual Lyα absorption systems found are labeled alphabetically in order of increasing heliocentric recession velocity. A detailed treatment of the Galactic absorption lines will be presented elsewhere (Shull, Penton, & Stocke 1995a); here we discuss only the Lyα forest lines. Since very few strong Galactic absorption lines (i.e., only the N v and S II lines mentioned above) are found in this spectral range and since the wavelengths of any potential Galactic interstellar absorption lines are very accurately known (Morton 1991) using the wavelengths of the strong S II lines as zero points, the confusion between Lyα lines and metal lines is minimal.

Even after the Lucy deconvolution of each spectrum was performed (only used for evaluating line widths of definite absorption lines), the derived velocity widths of the strong Galactic S II absorption lines in all three spectra exceed the expectations of ~ 30 km s^{-1} resolution for the pre-COSTAR capabilities of the G160M + LSA. The reasons for this are unclear, but we suspect that telescope wobble during individ-
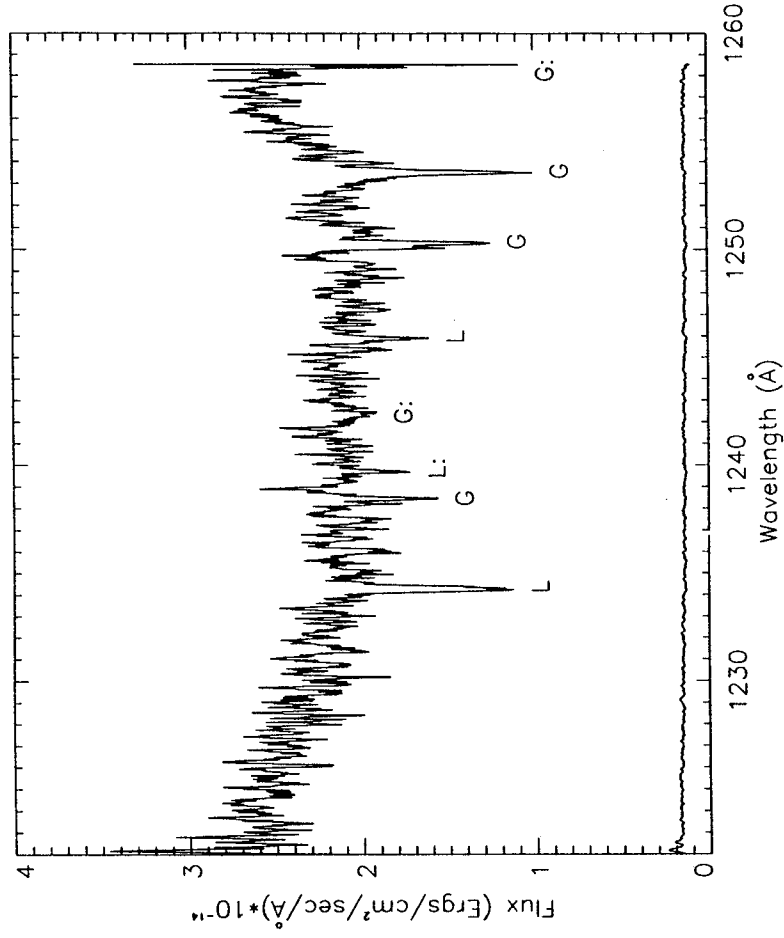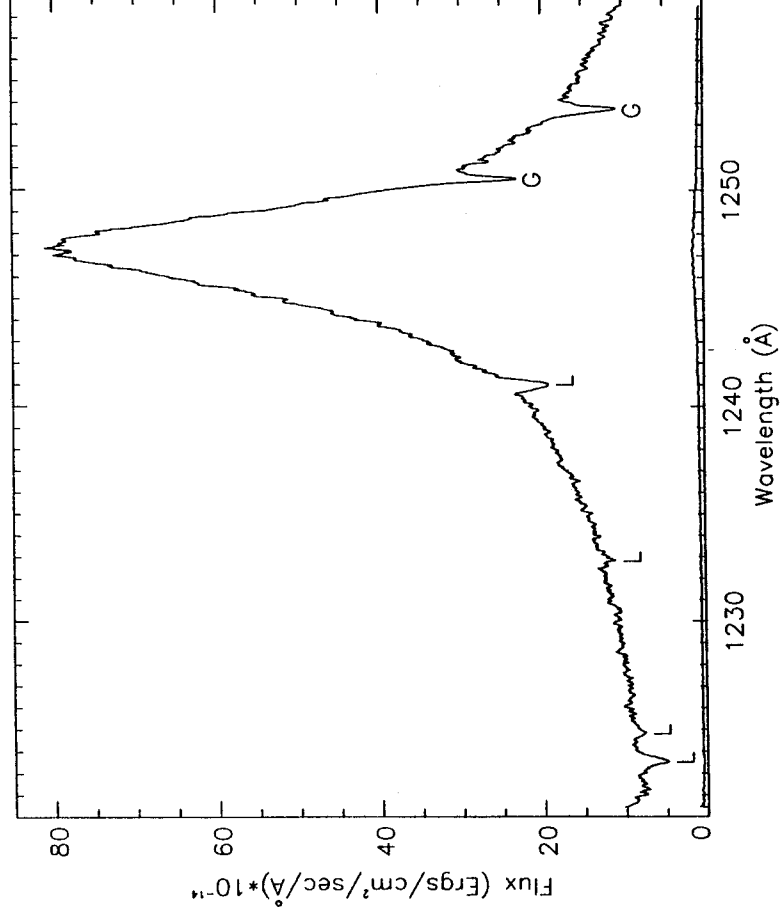
FIG. 1.—*HST*/GHRS + G160M spectra of three bright AGNs behind nearby galaxy voids. (*a*) Mrk 501, (*b*) Mrk 335, and (*c*) I Zw 1. The spectrum of I Zw 1 was not a complete observation as scheduled, owing to technical problems. The details of each individual spectrum are discussed in the text. Galactic absorption lines are marked "G," and are due to N v $\lambda\lambda 1238$, 1242 and S ɪɪ $\lambda\lambda 1250$, 1253. Definite Lyα absorption lines are marked with an "L"; those marked "L" are tentative Lyα lines. The error spectrum based upon photon statistics alone is shown at the bottom.
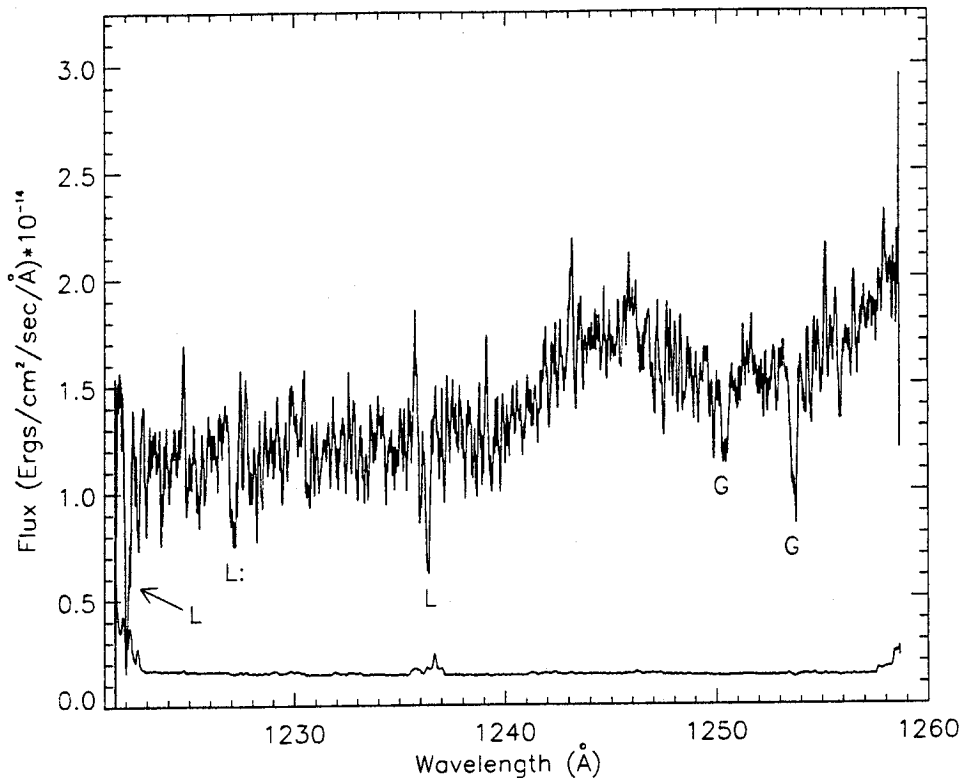
FIG. 1c

ual FP-split exposures and/or incorrect on-board Doppler compensation during some of the exposures (Hulbert 1993) is at fault. This problem is particularly apparent in the spectrum of Mrk 335 (see Fig. 1). The result of this analysis is that all Lyα lines but one are unresolved by these observations. The limiting FWHM for the Mrk 335, Mrk 501, and I Zw 1 definite Lyα lines are $< 50, 40$, and 40 km s^{-1} respectively. The one resolved Lyα absorption line is system D (6280 km s^{-1}) in the Mrk 335 spectrum, which has a measured FWHM of 60 ± 20 km s^{-1}. The Lucy deconvolved spectrum of Mrk 335 appears to show two largely overlapping Lyα lines at the location of system D; the weaker line has an equivalent width of the order of one-third of the total shown in Table 2 and is blueward of the position of the stronger line (and of the position in Table 2) by ~ 40 km s^{-1}. The post-COSTAR GHRS + G160M is capable of resolving these lines and determining their individual Doppler widths and equivalent widths.

Because these observations did not resolve the Lyα absorption lines in velocity, we assume a value of the Doppler parameter $b = 30$ km s^{-1} in order to calculate column densities. This value is typical of high-z Lyα forest clouds and is close to the median value of ~ 26 km s^{-1} found by Rauch et al. (1993) in a recent study. The line-center optical depth of Lyα is then $\tau_0 = 0.253 N_{13}/b_{30}$, where N_{13} is the column density in units of 10^{13} cm^{-2} and b_{30} is the Doppler parameter in units of 30 km s^{-1}. Since, by the linear approximation, the minimum column density of Lyα is related to the equivalent width by $W_\lambda^{lin} = (54.5 \, \text{mÅ}) N_{13}$, it is unlikely that any of the Lyα lines detected in these observations are saturated. For example, by the above expressions, the largest equivalent width Lyα line in Table 2 (I Zw 1 system A) has an optical depth $\tau_0 \approx 1$. Therefore, we list these minimum column densities in column (3) of Table 2 as

a good approximation of the actual column densities of these detections.

2.1. Mrk 501

The spectrum of Mrk 501 was obtained when this BL Lac object was close to its median flux level as observed for the last 15 years with the *IUE* satellite (Edelson et al. 1992). Thus, the S/N and limiting equivalent width (~ 40 mÅ) are near the values expected in the planning of this project. The continuum bump at the red end of the Mrk 501 spectrum is weak Lyα emission, which is expected at a wavelength of 1257 Å based upon the optical absorption-line redshift for this object ($z = 0.034$). Based upon detecting only two-thirds of the line profile, we estimate that the Lyα emission has $W_\lambda \sim 1$ Å and FWZI ~ 1400 km s^{-1}. This is the first detection of broad or narrow emission line gas in this BL Lac object. While weak emission lines with $W_\lambda \leq 10$ Å have been detected in the spectra of several BL Lac objects (e.g., Stickel, Fried, & Kuhr 1993), no sensitive survey for the presence of Lyα emission has been conducted for these rare objects, so the frequency of occurrence is presently unknown.

Also at the red end of the spectrum is a possible detection of the blue wing of the Galactic S II 1259.519 Å absorption line. The red component of the N v absorption doublet at 1242.804 Å may also be present (see Fig. 1), but it is not statistically significant in our data. It is possible that very weak N v 1238, 1242 Å Galactic emission is present (2 σ level) in this spectrum at approximate LSR velocities of −165 and +135 km s^{-1}. A similar emission feature may be present just blueward of the S II 1250 Å absorption line. However, whether real, instrumental, or due to photon or systematic noise, their presence makes the measurement of potential weak absorption features diffi-

TABLE 2

DETECTED ABSORPTION LINES

Object/System Designation (1)	Wavelength[a] (Å) (2)	W_λ(mÅ)/ log N(H I)(cm^{-2}) (3)	Significance Level (σ) (4)	Identification Velocity[a] (5)
Mrk 335:				
A............	1223.65	170/13.50	31.2	Lyα; 1970 km s^{-1}
B............	1224.97	73/13.13	11.9	Lyα; 2290 km s^{-1}
C............	1232.99	26/12.68	5.1	Lyα; 4270 km s^{-1}
D[b]	1241.12	140/13.41	46.9	Lyα; 6280 km s^{-1}
	1250.57	144	89.0	S II Galactic
	1253.79	196	61.6	S II Galactic
Mrk 501:				
A............	1234.58	154/13.45	13.7	Lyα; 4660 km s^{-1}
	1238.76	42	4.0	N V Galactic
B:[c]	1240.01	36/12.82	3.4	Lyα; 6000 km s^{-1}
C............	1246.19	48/12.94	4.6	Lyα; 7530 km s^{-1}
	1250.56	116	11.2	S II Galactic
	1253.79	168	16.2	S II Galactic
I Zw 1:				
A............	1222.21	240/13.64	5.1	Lyα; 1610 km s^{-1}
B:[c]	1227.26	95/13.24	3.8	Lyα; 2860 km s^{-1}
C............	1236.50	120/13.34	4.8	Lyα; 5140 km s^{-1}
	1250.55	106	4.2	S II Galactic
	1253.83	135	5.4	S II Galactic

[a] These are heliocentric wavelengths and velocities obtained by assuming that the S II lines are at the LSR.

[b] System D may consist of two individual Lyα absorptions separated by 40 km s^{-1}. The velocity of the absorption minimum is listed here, and the equivalent width is the total of the two.

[c] A colon indicates "tentative" absorption-line detections (3–4 σ).

cult in this spectrum in the 1237–1243 Å range. One definite and one tentative Lyα forest line (systems B and C) associated with a void in the distribution of CfA galaxies are present in this spectrum at $cz = 6000$ and 7530 km s^{-1} respectively. Other continuum dips in this region (e.g., at 1236.0 and 1245.4 Å) are below the 3 σ significance level. Additional weak absorption may be present just redward of the Galactic S II 1250 Å line, but the presence of the Galactic absorption makes its reality difficult to judge.

Although we did not definitely detect electronic pattern noise in this spectrum, the measured continuum errors somewhat exceeded the noise expected on the basis of photon statistics alone (shown at the bottom of Fig. 1a). If we had used the error vector in Figure 1a, the statistical significance of all absorption lines would have been somewhat higher; by that analysis the system B and C lines (the "void absorbers") had significance evels of 4.8 and 6.5 σ, respectively.

2.2. Mrk 335

The spectrum of Mrk 335 was obtained when this object was at its maximum observed flux based upon *IUE* SWP spectra (Penton, Shull, & Edelson 1994). Although the presence of extremely strong Lyα emission in this spectrum would seem to enhance detectability of absorption features at velocities approaching 7500 km s^{-1}, the difficulty in accurately fitting the steep continuum gradient on the blue wing of Lyα partially offsets this advantage. The strong S II 1259.519 Å Galactic absorption line may be present at the extreme red end of this spectrum as in Mrk 501. The error spectrum shown for this object in Figure 1 is based upon photon statistics alone. However, there is evidence for some pattern noise in this spectrum which increases the actual noise level by $\sim 2^{1/2}$. The statistical significances listed in Table 2 were computed using these higher error estimates. As mentioned above, this spec-

trum suffered from a degraded resolution from unknown causes which leaves all lines unresolved at ≤ 50 km s^{-1}, except for the Lyα absorption in system D. The system D line is clearly broadened more than the 1253 Å S II Galactic line, and the Lucy deconvolution of this spectrum separates this feature into two components. Despite this, the system D absorption will be treated as a single system with the parameters listed in Table 2 for the analysis herein.

2.3. I Zw 1

The spectrum of I Zw 1 contains a moderately strong, broad emission line identified as C III λ1175, which has been seen in this quasar at some epochs with the *IUE*. At the red end of this spectrum the continuum is beginning to rise because of the blue wing of Lyα. At the extreme blue end of the spectrum is a definite Lyα forest line at ~ 1600 km s^{-1}. Because we detect continuum on either side of this feature, we believe that the continuum fit is adequate and the line definitely detected. While the onset of the damping wing of Lyα absorption in the Milky Way is expected to reduce the continuum level by $\sim 10\%$ at this wavelength, it should not affect our measurement of this sharp feature because it is so broad (see Weymann et al. 1995).

Both of the definite Lyα absorption lines discovered in this spectrum are in regions of slightly higher noise due to less than 5% sensitivity "blemishes" on the photocathode according to the automated GHRS flagging software. The exclusion of the flagged data increased the noise somewhat (see Fig. 1c) but did not alter the statistical significance levels of these two absorptions; if no data were excluded, these lines would still have a significance level higher than 4 σ. To be conservative, we have shown the spectrum of I Zw 1 and tabulated the absorption-line data in Table 2 with these data excluded.

Because of *HST* technical difficulties, this observation was

TABLE 3

NEAREST GALAXY NEIGHBORS TO Lyα CLOUDS

Target System	cz_0 (km s^{-1}),[a] EW (mÅ)	Nearest Galaxy	cz_0 (km s^{-1}),[a] $M(B)$	$\delta\Theta$ (deg) $M(B)$ Limit	δr^b (h_{75}^{-1} Mpc)
Mrk 335:					
A.......	2185, 171	NGC 7817	2520, −19.8	0.80, −17.0	0.67
B	2510, 73	NGC 7817	2520, −19.8	0.80, −17.0	0.45
C	4490, 26	0000.8 + 2150	4670, −17.9	2.0, −18.4	2.2
D^c	6490, 140	0003.6 + 1928	6150, −17.7	0.46, −19.2	0.85
Mrk 501:					
A.......	4870, 154	1651.0 + 3927	4835, −19.0	0.45, −18.6	0.51
B:	6210, 36	IC 1221	5690, −19.7	7.6, −18.9	10.5
C	7740, 48	1709 + 3941	7810, −19:	3.3, −19.6	5.9
I Zw 1:					
A.......	1740, 240	NGC 63	1300, −18.6	8.7, −15.7	3.1
B:	3000, 95	A0054 + 1005	2890, −17:	2.5, −17.2	1.7
C	5280, 120	0052.2 + 1325	5560, −16.2	1.0, −18.7	1.3

[a] Galactocentric velocities.

[b] " Retarded Hubble flow model;" see text.

[c] System D may consist of two individual Lyα absorptions separated by 40 km s^{-1}. The velocity of the absorption minimum is listed here.

only partially completed, with the result that the S/N in Figure 1c is well below that desired for this project. This target will be reobserved during cycle 4, as will our final target in this program, the BL Lac object Mrk 421.

Although the continuum strength in each object varies somewhat with wavelength, the limiting equivalent width varies much more from object to object. Therefore, we make no attempt in this current paper to construct a detailed absorption-line selection function or a statistically complete sample of absorption lines based upon the current data.

3. THE Lyα FOREST, GALAXIES, SUPERCLUSTERS, AND VOIDS

Prior to the observations, we used the CfA and Arecibo wide-angle galaxy survey results to determine the location along each sight line of superclusters and voids. Having this information in advance was the primary reason that these particular sight lines were chosen for study. These targets are the brightest targets behind well-defined cosmic voids based upon these survey data and so possess a larger fraction of their total sight line through void than would random sight lines. The path lengths through supercluster and void probed by this project thus far are nearly equal: 11,800 and 11,400 km s^{-1}, respectively. However, the definite Lyα absorption-line detections do not reflect the nearly equal path lengths, since seven absorption lines were detected in superclusters and only one was clearly found within the boundaries of a void, system C in the Mrk 501 spectrum. Two other greater than 4 σ lines, system A in I Zw 1 and system B in Mrk 335, are near supercluster/void boundaries but are within the supercluster regions along these sight lines defined by us prior to the HST observations. One of the two 3–4 σ lines (system B in Mrk 501) is also in a void region.

If Lyα lines are uniformly distributed, as suggested by the absence of power at any scale in their observed two-point correlation function at high z (e.g., Rauch et al. 1993), the chance binomial probability of detecting only one absorption line out of eight in voids thus far in our survey is ~3%. If we include the weaker (3–4 σ) Lyα lines, the statistics become two out of 10 in voids, which has ~5% binomial probability to arise by chance. Clearly, data on more sight lines are needed to be definitive on this point, but for now we assert that (1) the

detection of one and possibly two Lyα lines within galaxy voids means that these voids are not entirely devoid of matter despite the absence of even low-luminosity galaxies (Szomoru et al. 1994), and (2) there is nevertheless already some statistical evidence that even the low-mass Lyα clouds seem to avoid the voids. We elaborate on the evidence for the latter statement in the remainder of this section.

Based on the galaxy redshift data from the CfA merged galaxy redshift catalog (Huchra 1993), Figure 2 shows the distribution of galaxies within 10° of our three sight lines in the form of "pie diagrams" in both right ascension and declination.[6] Because these sight lines are within the CfA or Arecibo galaxy survey regions, most of the galaxies are from those surveys, which are complete to $V = 15.5$. Some fainter galaxies are also included in the CfA catalog in these regions. In Figure 2 the sight line is the dashed line in the middle of each plot with the position of the AGN target marked with a large circle. The positions of the Lyα clouds are marked with smaller circles (the middle-sized circles being the definite, $\geq 4\sigma$, detections). The radial coordinate in each plot is the Galactocentric redshift, as are all velocities quoted hereafter (e.g., the "void absorber" in the Mrk 501 sight line at $cz = 7530$ km s^{-1} heliocentric will hereafter be referred to by its Galactocentric velocity of 7740 km s^{-1} as shown in Table 3). Because these wedges project all galaxies within 10° onto the plane of the plot, for a galaxy to be along the sight line it must be along the dashed line in both wedges.

The visual impression supplied by these wedges is that most Lyα lines are associated with supercluster structures (i.e., superclusters or "strings" of galaxies) in the large-scale galaxy distribution. For example, in Figure 2b the nearer two absorbers are within the Local Supercluster, while the two more distant absorbers are in the Perseus-Pisces supercluster. In Figure 2a the nearest absorber is coincident with a thin string of galaxies that separates two much larger regions of void. Despite this visual impression of association with galaxy supercluster structures on the large scale, there is no evidence

[6] Because the Mrk 501 sight line is near the eastern edge of the CfA survey, we obtained 20 additional redshifts of galaxies at R.A. > 17^h from the ongoing galaxy redshift survey being conducted at CfA to verify that the voids along the Mrk 501 sight line extend well beyond 17^h (J. P. Huchra 1994, private communication).
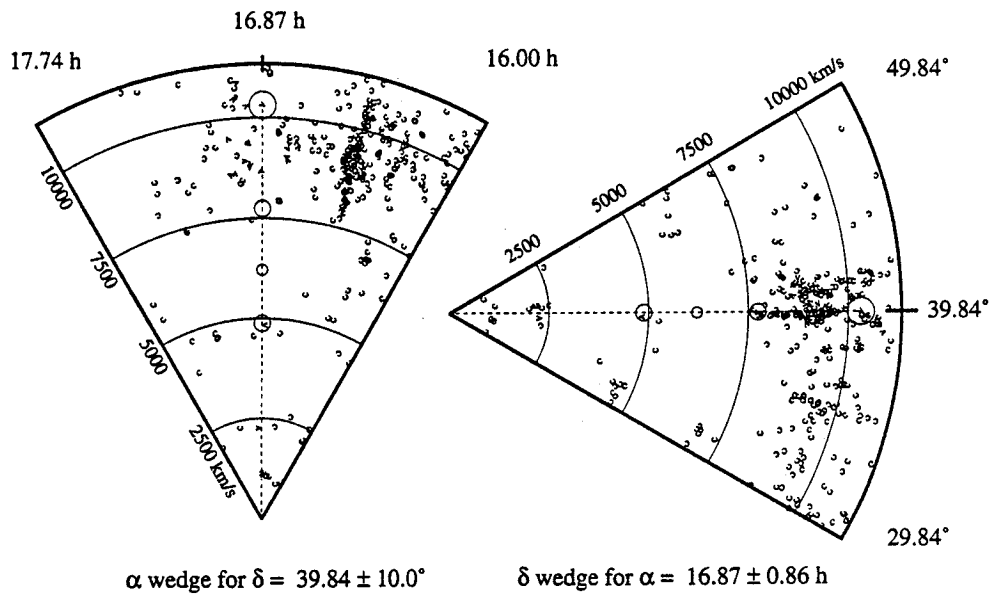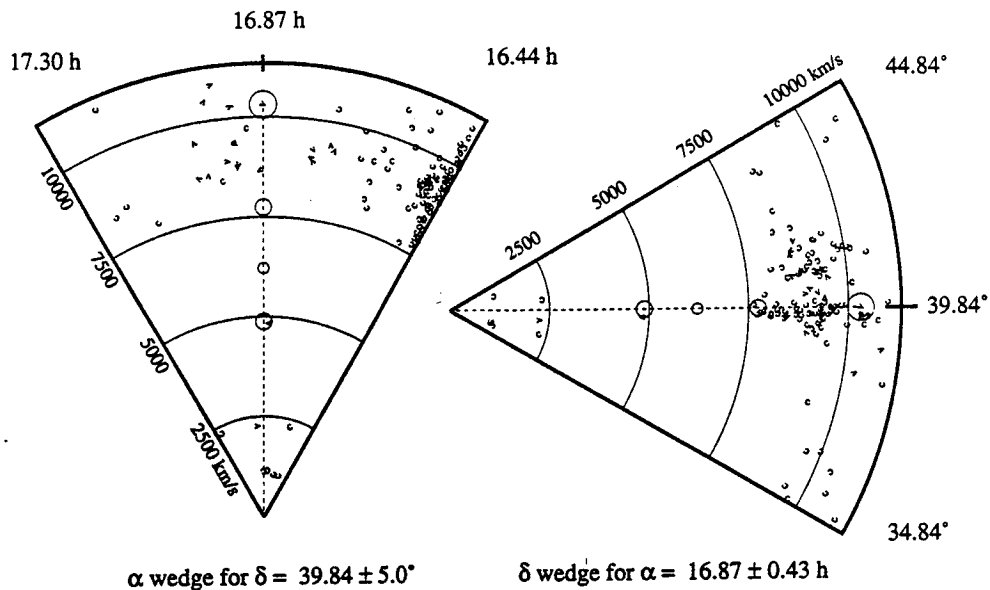
MRK 501
10° wedge

16.87 h

17.74 h

16.00 h

49.84°

10000 km/s

16.00 h

10000

7500

5000

2500 km/s

7500

5000

2500

39.84°

29.84°

α wedge for δ = 39.84 ± 10.0°   δ wedge for α = 16.87 ± 0.86 h

FIG. 2a

MRK 501
5° wedge

16.87 h

17.30 h

16.44 h

44.84°

10000 km/s

10000

7500

5000

2500 km/s

7500

5000

2500

39.84°

34.84°

α wedge for δ = 39.84 ± 5.0°   δ wedge for α = 16.87 ± 0.43 h

FIG. 2b

FIG. 2.—"Pie diagrams" for the three sight lines. The wedges in right ascension (α) and declination (δ) are marked along the pie's edge and are 10° wide (5° width in [b]) in the opposite coordinate. The coordinate along the slice of the pie is Galactocentric redshift in km s^{-1}. The dashed line in each diagram marks the sight line, with the large circle indicating the position of the AGN target. The smaller circles indicate the positions along the sight line of the Lyα absorbers; the middle-sized circles are the definite detections, and the smallest circles are the tentative detections. Each symbol "c" is an individual galaxy in the merged CfA redshift catalog; the orientation of the "c" for each galaxy is conserved between the two plots. The "v" symbols indicate CfA catalog galaxies within 2° of the sight line and are also oriented consistently between the right ascension and declination plots. Galaxies at cz < 1500 km s^{-1} have been deleted from these plots.
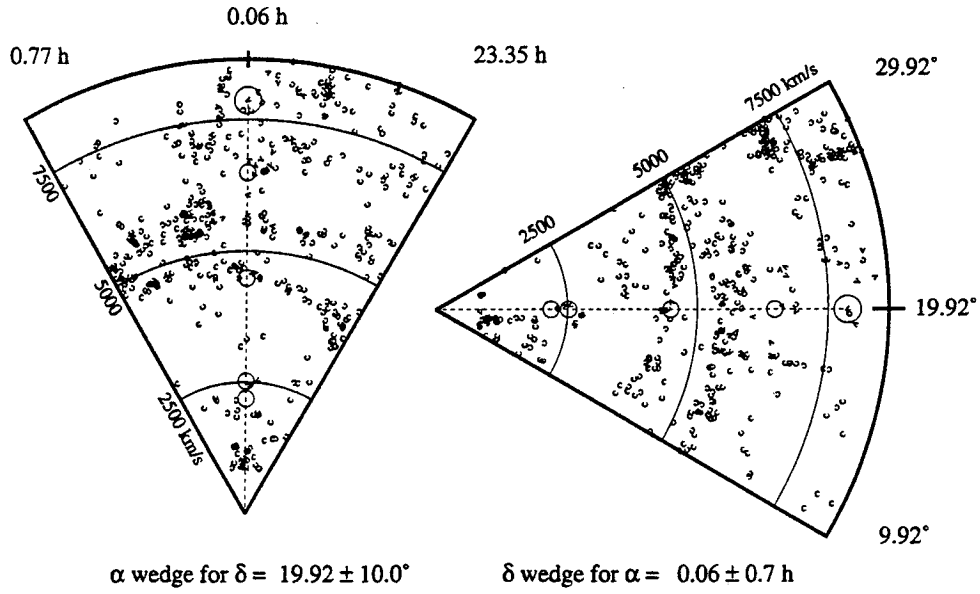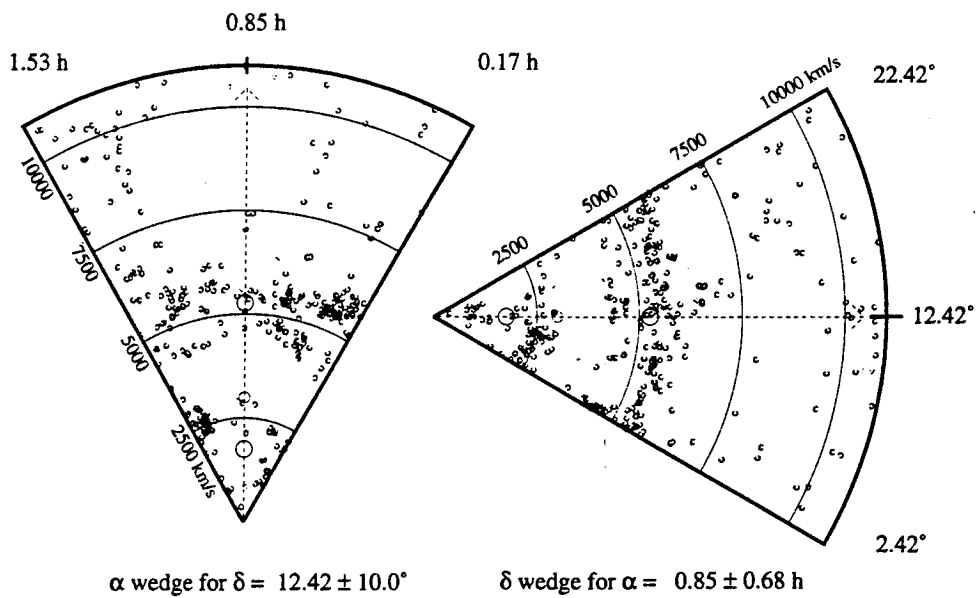
MRK 335
10° wedge

0.06 h

0.77 h   23.35 h   29.92°

7500 km/s

7500

5000

5000

2500

2500 km/s   19.92°

9.92°

α wedge for δ = 19.92 ± 10.0°   δ wedge for α = 0.06 ± 0.7 h

FIG. 2c

I ZW 1

0.85 h

1.53 h   0.17 h   10000 km/s   22.42°

10000

7500

7500

5000

5000

2500

2500 km/s   12.42°

2.42°

α wedge for δ = 12.42 ± 10.0°   δ wedge for α = 0.85 ± 0.68 h

FIG. 2d

of individual galaxy–Lyα cloud associations on the small scale. Specifically, the closest cloud-galaxy separation in our sample is 470 kpc, and there are some absorption lines with no known galaxies within 2° or well over 1 Mpc at typical cloud redshifts (see below).

In Figure 2 we show 5° wedges for the Mrk 501 sight line, in order to stress how few galaxies lie close to this sight line. The Lyα cloud designated system A manages to locate the only galaxy within 2° of this sight line between the Local Supercluster and the Great Wall, while the other two absorptions are in extremely empty regions. Notice that, while many symbols representing galaxies appear to be close to the 7740 km s^{-1} absorption system, in fact there are none closer than almost 6 Mpc. Most of the symbols marking galaxies along the horizontal line in the declination plot are members of Abell 2199, which, although at the same declination as Mrk 501, is centered at R.A. 16^{h}27^{m}0, about 10 Mpc to the west. Directly along the sight line, the nearest galaxies are ~16 h_{75}^{-1} Mpc in the background in what is known as the Great Wall. The 6210 km s^{-1} absorber is near the middle of this same void, with a nearest known galaxy more than 10 Mpc away. The positions of both these absorbers are within the area identified by Slezak, de Lapparent, & Bijaoui (1993) as a "significant void" using a "wavelet" technique on the CfA survey data. Although the Mrk 501 sight line is close to the eastern edge of the CfA survey strip, which ends at 17^h R.A., the merged redshift catalog data shown in Figure 4 clearly shows that the void, which extends from 4700 to 8700 km s^{-1}, also extends considerably east of 17^h. These two Lyα clouds (one a definite detection at 4.6 σ, one tentative at 3.4 σ) are well within this void.

We have used the merged CfA redshift catalog to determine the distances to the nearest galaxies from each of the absorption lines detected in our spectra. This was done in a manner similar to that presented in M93 for two different cases: "pure Hubble flow" and "retarded Hubble flow." In the former model, a radial distance between galaxy and cloud was obtained using the actual difference between galaxy and cloud velocities (δv) scaled by the Hubble parameter (i.e., $\delta v H_0^{-1}$). In the latter model, $|\delta v| < 300$ km s^{-1} was assumed to place the galaxy and cloud at the same radial distance from us, while a radial distance of $(\delta v - 300)H_0^{-1}$ was assumed for $|\delta v| > 300$ km s^{-1}. This "retarded Hubble flow" model allows for some cloud peculiar velocity relative to the galaxy in an amount comparable to the escape speed from a small galaxy. A Hubble constant of $H_0 = 75 \, h_{75}$ km s^{-1} Mpc^{-1} is assumed, and measured values are scaled as h_{75} where required. Tangential distances on the sky are scaled as h_{75}^{-1}, except for absorptions within the Local Supercluster, where the galaxy distances from the Tully (1988) Nearby Galaxies Catalog were adopted.

In Table 3 we list the nearest-galaxy information for each of the eight definite Lyα lines and the two tentative ones found in our spectra. All the velocities are Galactocentric, and the total cloud-galaxy distances assume the "retarded Hubble flow" model above. The limiting galaxy absolute magnitude for each absorption system has been determined using the limiting magnitude $V \approx 15.5$ for the CfA and Arecibo surveys, even if, in some cases, fainter objects have measured redshifts in these areas—e.g., some of the nearest galaxies to Lyα clouds listed in Table 3. Because these absorption systems are very near by, the limiting magnitudes for galaxies surveyed along these sight lines are comparable to or less luminous than limiting galaxy magnitudes in quasar fields with low-z metal absorption systems (cf. Steidel 1993; Lanzetta et al. 1994) as well as the

higher redshift Lyα absorption systems in the 3C 273 sight line (M93), where significantly deeper optical work was required to identify galaxies and obtain redshifts. We are currently undertaking pencil-beam optical galaxy surveys as well as redshifted 21 cm emission surveys in these fields to improve these limiting magnitudes significantly. In one such search for fainter galaxies, reported in § 4, we failed to detect low-luminosity galaxies closer to the Mrk 501 Lyα clouds than any listed in Table 3.

The nearest-galaxy data are shown in histogram form in Figure 3, compared with similar data for all of the M93 Lyα absorbers in the 3C 273 sight line and two of the three lowest redshift Lyα clouds in the sight line to PKS 2155−304 (Bruhweiler et al. 1993). The nearest galaxies to the 3C 273 absorbers are based upon the optical galaxy multiobject spectroscopy data presented in M93 converted to $H_0 = 75$ km s^{-1} Mpc^{-1} and the "retarded Hubble flow" model used here. Two of the three lowest z absorption systems in the PKS 2155−304 sight line (5145 and 17,100 km s^{-1}) were observed using the VLA DnC configuration at the frequencies of the redshifted H I 21 cm emission line (Carilli et al. 1995) over a region 0.5 or 1.5 Mpc in radius around the sight line for the two Lyα cloud redshifts above. Limiting sensitivities were sufficient to detect normal gas-rich galaxies at these redshifts, and the galaxies found in these observations were used in Figure 3. Because of technical problems, only velocities greater than the velocity of a third Lyα absorption line at 16,500 km s^{-1} along this sight line were observed, so we cannot quote a nearest-neighbor distance for this third system with confidence. No nearer galaxies are known to this sight line at the Lyα cloud redshifts based upon optical work, but galaxy redshift survey work near PKS 2155−304 is not yet extensive. Details of the redshifted H I observations near PKS 2155−304 will be presented in Carilli et al. (1995). Only those 27 Lyα clouds which have had their environs well surveyed for galaxies are included in Figure 3. Throughout the remainder of this paper we term these 27 clouds the "GHRS Lyα sample."

The primary motive for displaying Figure 3 is to expand the qualitative understanding of the local Lyα clouds obtained from the present work and apply it to the 3C 273 and PKS 2155−304 absorbers and thus to local Lyα clouds in general. Certainly the two distributions are quite similar (a Kolmogorov-Smirnov [KS] test yields a 96% probability that these two distributions are consistent with being drawn from the same parent population), suggesting that the inferences from the current data are general. Specifically, the fact that the nearest galaxy neighbors to Lyα clouds are often ≤2 Mpc away is consistent with these clouds being associated with superclusters or galaxy "strings." These clouds are not necessarily associated with individual galaxies, since the closest cloud/galaxy associations in the GHRS Lyα sample are ~250 kpc distant, and half of the nearest-neighbor distances are greater than 1 Mpc. These very large cloud-galaxy separations are difficult to reconcile with models that associate Lyα clouds with the extended gas envelopes of individual galaxies (e.g., Bahcall & Spitzer 1969; Maloney 1992; Dove & Shull 1994; Mo 1994; § 5 below). Not only is it difficult to construct plausible gas distributions to account for these Lyα clouds (see § 5), but on scales of ≥1 Mpc it is not obvious sometimes which galaxy is the nearest neighbor.

Most (19 out of 27) Lyα lines detected thus far are likely associated with supercluster structures, with nearest-neighbor galaxies less than 2 Mpc away. Four Lyα clouds (nearest neigh-
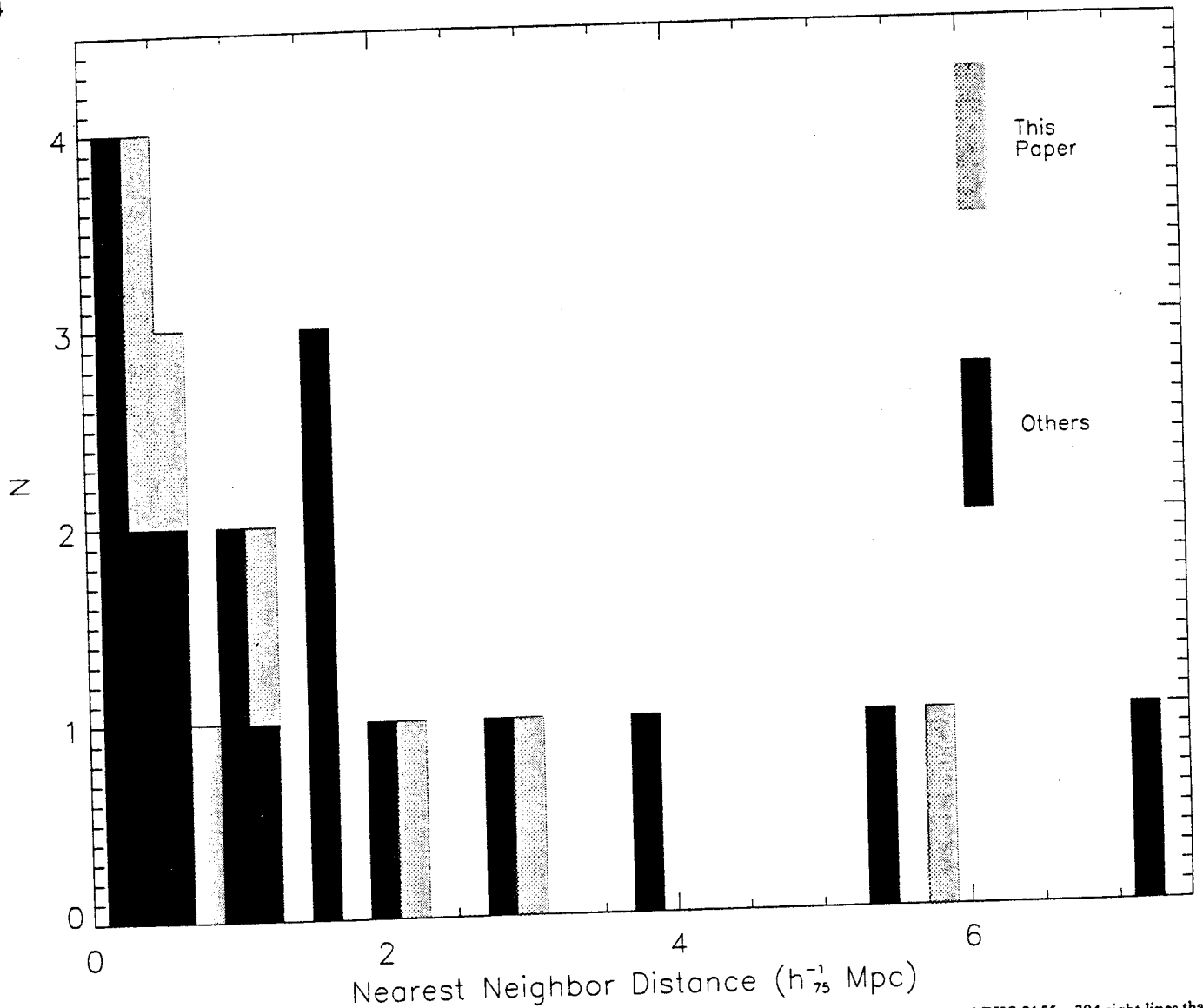
FIG. 3.—Histogram of nearest-neighbor statistics for the definite Lyα clouds discovered herein and those found in the 3C 273 and PKS 2155—304 sight lines that have been well studied for surrounding galaxies. Nearest-neighbor distances have been calculated assuming the "retarded Hubble flow" model described in the text. There is no statistical difference (96% probability) between these two samples in nearest-neighbor proximity, so we combine them into a single "GHRS Lyα sample."

bors 2–3.5 Mpc away) are at locations far enough from galaxies to make their association with supercluster structures questionable. Finally, four out of 27 clouds, with nearest neighbors more than 3.5 Mpc away, are likely associated with voids and *not* with galaxies. Interestingly, the three Lyα clouds along the 3C 273 sight line, which lie in areas of space comparably vacant to the one Lyα cloud confidently identified with a void in our sample, are in a clump at similar redshifts: $z = 0.06$–0.07. The pencil-beam redshift survey accomplished by M93 shows a large concentration of galaxies just beyond these redshifts; this is similar to the geometry of galaxies locally where voids are immediately in front of the Great Wall as seen from our location. The redshift range of these three absorption systems along the 3C 273 sight line should be investigated in greater detail for galaxies. Based upon the absorption-line study reported here, we identify this complex of three absorption lines as also associated with a void. If this is the case, their clustering in velocity may *not* be related to a clustering of

galaxies [unlike the Virgo supercluster ($z < 0.01$) and Great Wall ($0.02 < z < 0.035$) absorption systems in this same sight line].

M93 used the 3C 273 Lyα cloud locations and the galaxy locations found in their pencil-beam redshift survey to construct cloud-galaxy and galaxy-galaxy two-point correlation functions along this sight line. Their analysis shows that local Lyα forest lines are not uniformly distributed through space, as expected on the basis of the high-z data. But neither do these clouds cluster with galaxies as strongly as galaxies cluster with each other. M93 concluded that while Lyα clouds cluster weakly with galaxies, there may be some evidence suggesting that these clouds avoid the richest galaxy regions and could even be destroyed by some process in those regions (see also Mo & Morris 1994; Rees 1988). The latter inference is based upon the absence of close cloud-galaxy associations in the 3C 273 sight line; the closest cloud-galaxy association M93 found was $\sim 250\ h_{75}^{-1}$ kpc, which creates an apparent deficit in the

two-point correlation function amplitude for cloud-galaxy pairs compared with galaxy-galaxy pairs at less than 500 kpc.

We confirm most of the M93 results using a somewhat different analysis of the GHRS Lyα sample. Using the CfA redshift survey, we have positioned randomly nearly 2200 simulated Lyα clouds along 1000 sight lines within the boundary of a complete CfA survey region: 1596 galaxies within $08^h5 \leq$ R.A. $\leq 17^h5$, $26°5 \leq$ decl. $\leq 32°5$, 1500 km s$^{-1} \leq cz \leq 10{,}500$ km s^{-1}. These simulated clouds were placed at a mean rate of 1 cloud per 3500 km s^{-1}, consistent with the observed cloud density in the GHRS Lyα sample. Distances from these simulated cloud positions to the nearest galaxy in the CfA survey were then determined using the two models (pure and retarded Hubble flow) for computing radial distance described above. We also simulated a "proximity" effect (Bechtold 1993; Bajtlik 1993) for Seyfert galaxies within the CfA survey by removing all Lyα clouds within 1 Mpc of any galaxy noted as a Seyfert 1 or 2. Including the proximity effect made no statistically discernible change in the overall nearest-neighbor distributions of the simulated, randomly placed clouds.

The results of the Monte Carlo simulation for the "retarded Hubble flow" model are shown in Figure 4. The distances from CfA galaxies to their nearest galaxy neighbors are plotted as well and are, of course, consistent with the local two-point correlation function for galaxies, since this is one of the primary data sets from which this function is determined (Peebles 1993, chap. 19). Also plotted is the actual distribution of nearest neighbors for the 27 clouds in the GHRS Lyα sample. Clearly, the local Lyα clouds are not randomly located with respect to galaxies; a KS test shows that this difference is statistically significant at higher than the 99.7% confidence

level. Nor do the local Lyα clouds cluster as strongly as the galaxies cluster with each other (>99.99% confidence level). The results of the "pure Hubble flow" model are quite similar and equally statistically significant. In this comparison we are using the CfA survey galaxy positions to characterize the distribution of galaxies in general, and along these five sight lines in particular. Only one of the five sight lines (Mrk 501) actually passes through the CfA survey region.

While these data strengthen the M93 claim that Lyα clouds do appear to cluster weakly with galaxies, we cannot confirm their suggestion that Lyα clouds avoid the densest galaxy regions. Based upon Figure 4 and the size of the error bars on the cloud-galaxy two-point correlation function amplitude at less than 500 kpc (M93), we conclude that the current sample size of local Lyα clouds is not large enough to exclude the possibility of very close cloud-galaxy separations. The data also appear too sparse to evaluate the percentage of Lyα clouds due to extended galaxy halos and the percentage due to other sources (e.g., tidal tails, CDM "minihalos") as attempted by Mo & Morris (1994). We return to this point in § 5.

Recently, Lanzetta et al. (1994, hereafter L94) have used *HST* FOS spectra of bright quasars observed by the Key Project Team (Bahcall et al. 1993) to study the question of nearest galaxies to Lyα clouds at somewhat higher redshifts ($z = 0.1$–0.3). Because the best FOS data have wavelength resolutions of ~1 Å, the minimum detectable equivalent widths in the Key Project data are greater than 100 mÅ. The minimum equivalent width line used by L94 is ~400 mÅ, 3–10 times higher than the typical equivalent widths detected by the three GHRS studies used in our analysis. Some of the L94 Lyα absorptions have corresponding metal-line absorptions, and a few others lack data in wavelength regions where Mg II and
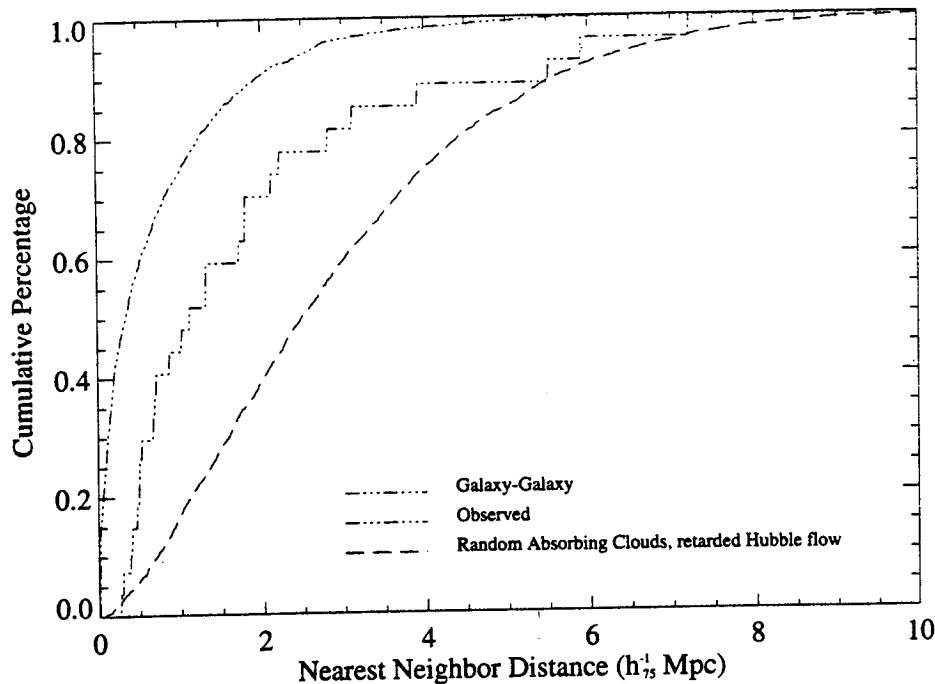

FIG. 4.—Cumulative distributions of nearest-neighbor statistics for the observed Lyα lines in the GHRS sample (*solid line*) and for two other distributions: the nearest-neighbor galaxy for all galaxies in the CfA complete survey region (*dash-dotted line*) and a large simulation (2637 clouds randomly placed along 1000 random sight lines) of randomly placed Lyα clouds within the CfA survey region (*dashed line*). The GHRS sample of 27 local Lyα clouds has a nearest-neighbor distribution statistically different from either the galaxy-galaxy or the random cloud-galaxy distributions at greater than 99.99% and greater than 99.7% probability levels, respectively.

Fe II absorptions would be present. Some of the Lyα clouds in the L94 sample do have observations in hand for both the C IV and the Mg II and Fe II spectral regions, and no metal-line absorptions are observed to modest limits (≤ 300 mÅ). Therefore, the clouds investigated by these authors may or may not be directly related to the clouds we have studied. At high z, it is currently debated whether there are two populations of H I clouds: those at high column density [$N(\text{H I}) \geq 10^{17}$ cm^{-2}] are metal-bearing and cluster like galaxies, while those at lower column densities [$N(\text{H I}) \leq 10^{17}$ cm^{-2}] could be metal poor and do not cluster (Sargent 1988; Tytler 1987). Recent evidence for a deficiency in the numbers of Lyα clouds at intermediate column densities (Kulkarni & York 1993; Meiksin & Madau 1992) supports the two-population hypothesis. But it is also possible that all Lyα clouds are a single population whose somewhat disparate properties are due only to the huge range in column density over which this phenomenon is observed (Tytler 1987).

Setting these concerns aside for the moment, we show in Figure 5 the distribution of equivalent widths versus impact parameters for the high equivalent width Lyα clouds from the L94 study and for the lower equivalent width clouds in the GHRS Lyα sample. The interesting result is that there is an apparent correlation (correlation coefficient $= -0.72$) between these two parameters which spans two orders of magnitude in both variables. While this result is suggestive that the high and low equivalent width systems are members of the same overall ensemble of clouds, all of which are related in some way to the bright, nearest-neighbor galaxy observed, we note that (1) the correlation at low equivalent widths ($W_\lambda < 300$ mÅ) is not nearly as tight as for the L94 clouds (if we consider the GHRS Lyα sample alone, the best-fit straight line has a slope half that

observed by L94 with a correlation coefficient of only -0.29 between these two parameters; see Fig. 5); and (2) the absence of Lyα clouds in the lower left-hand area of the plot is not yet statistically significant based upon the current sample size. If low equivalent width Lyα clouds were uniformly distributed with respect to galaxies (which is not precisely true), then the relative occurrence of clouds at impact parameters greater than or less than 300 kpc along random sight lines can be estimated using the random cloud positions in Figure 4. We would expect to find ~ 100 Lyα clouds at $r > 300$ kpc before the complete absence of Lyα clouds at smaller impact parameters becomes statistically significant. This is the same note of caution we expressed concerning the M93 inference that Lyα clouds avoid dense galaxy regions. More sight lines need to be observed before it can be argued that the low column density Lyα clouds obey the same relationship as the high column density clouds (L94) shown in Figure 5.

Even though the total number of local Lyα clouds found thus far by GHRS observations is small, we have divided the GHRS Lyα sample into two nearly equal groups above and below $W_\lambda = 100$ mÅ. The resulting cumulative distributions of nearest-galaxy neighbors are shown in Figure 6 together with the CfA galaxy and random cloud nearest-neighbor distributions from Figure 5. Although these Lyα samples are too small to draw any firm conclusion, we note that the higher equivalent width absorbers are distributed more like galaxies than the lower equivalent width absorbers, which are distributed in a manner statistically indistinguishable from clouds randomly placed with respect to galaxies. The $W_\lambda < 100$ mÅ absorbers have a distribution in Figure 6 that is consistent with the random cloud simulation at the 32% level. This is tantalizing evidence that at least some of the lowest equivalent width Lyα
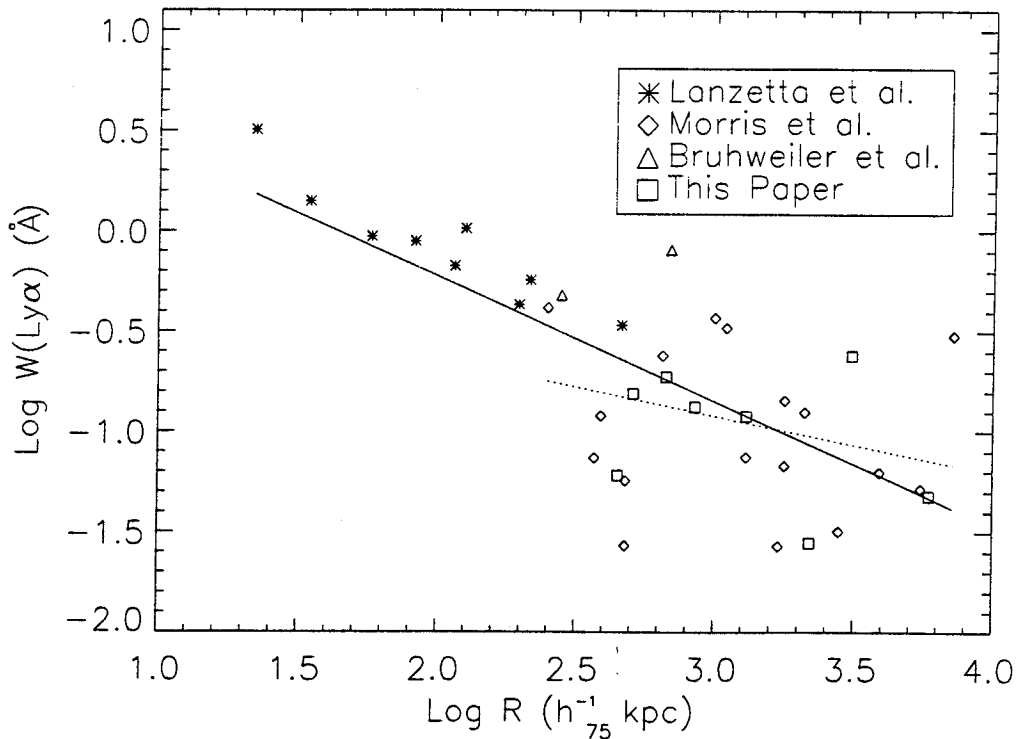

FIG. 5.—Lyα equivalent width versus nearest-galaxy distance for the GHRS Lyα sample and for the much higher equivalent width sample investigated by Lanzetta et al. (1994). The solid line is a linear regression fit to all the data shown (slope $= -0.62$; correlation coefficient, $R = -0.72$) and differs only marginally from the best fit to the Lanzetta et al. data alone. The dashed line is the best-fit line to the GHRS sample alone and is both significantly flatter (slope $= -0.29$) and less significant ($R = -0.29$) than the solid-line fit.
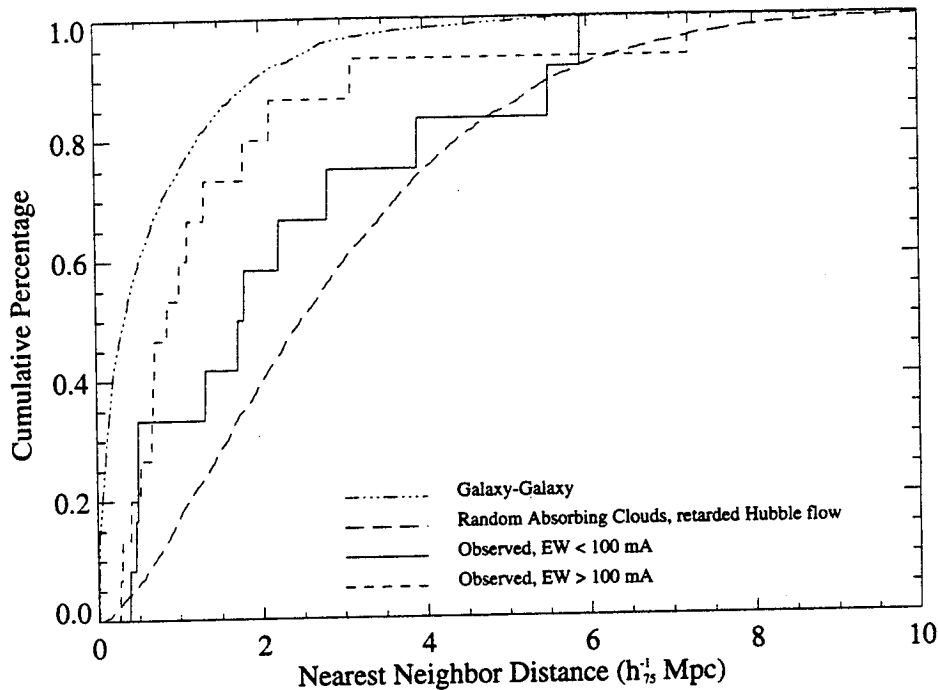
FIG. 6.—Cumulative distributions as in Fig. 4, except that the GHRS Lyα sample has been divided into low ($W_\lambda < 100$ mÅ) and high ($W_\lambda > 100$ mÅ) equivalent width systems. The low equivalent width systems have a distribution which is statistically indistinguishable from a random cloud placement with respect to galaxies (KS test probability of occurrence = 32%).

absorbers are true intergalactic clouds, unassociated with galaxies, while the higher equivalent width absorbers have some association with galaxies. However, we caution that the Lyα sample used in this analysis and the galaxy survey data used to determine nearest neighbors are not drawn from the same samples and so do not have well-defined selection functions, which are needed to remove subtle, likely distance-dependent, biases. The discovery of more very local Lyα absorptions at $W_\lambda \leq 100$ mÅ and a more systematic survey of their galactic environs are needed before a plausible multipopulation model for these clouds can be discussed in detail (Mo & Morris 1994).

4. THE "VOID" ABSORBER IN THE Mrk 501 SIGHT LINE

4.1. Search for Faint Optical Galaxies

Because of the importance of the absorption lines detected in the Mrk 501 sight line at $cz_0 = 6210$ and 7740 km s^{-1}, further

optical observations of this sight line were obtained to search for close neighboring galaxies. Figure 7 shows the Mrk 501 sight line with the BL Lac object itself situated at the center of the frame. The ~7' field of view corresponds to slightly over 100 h_{75}^{-1} kpc radius at the distance (103 h_{75}^{-1} Mpc) of the 7740 km s^{-1} void absorber. This image was obtained at the Canada-France-Hawaii 3.6 m telescope as part of a survey of the host galaxies and metagalactic environments of BL Lac objects (Wurtz, Stocke, & Yee 1995). Galaxies are detected in this frame down to $R \sim 22$. As part of the analysis of this field, a star-galaxy classifier called PPP (Yee 1991) was used to separate resolved galaxy images from stellar images and to obtain total magnitudes for all objects. Table 4 lists all of the galaxies with $B \leq 19$ mag on this image plus two additional galaxies observed spectroscopically. Table 4 lists the right ascension and declination offsets (arcsec) for each galaxy from

TABLE 4

GALAXIES IN THE FIELD OF MARKARIAN 501

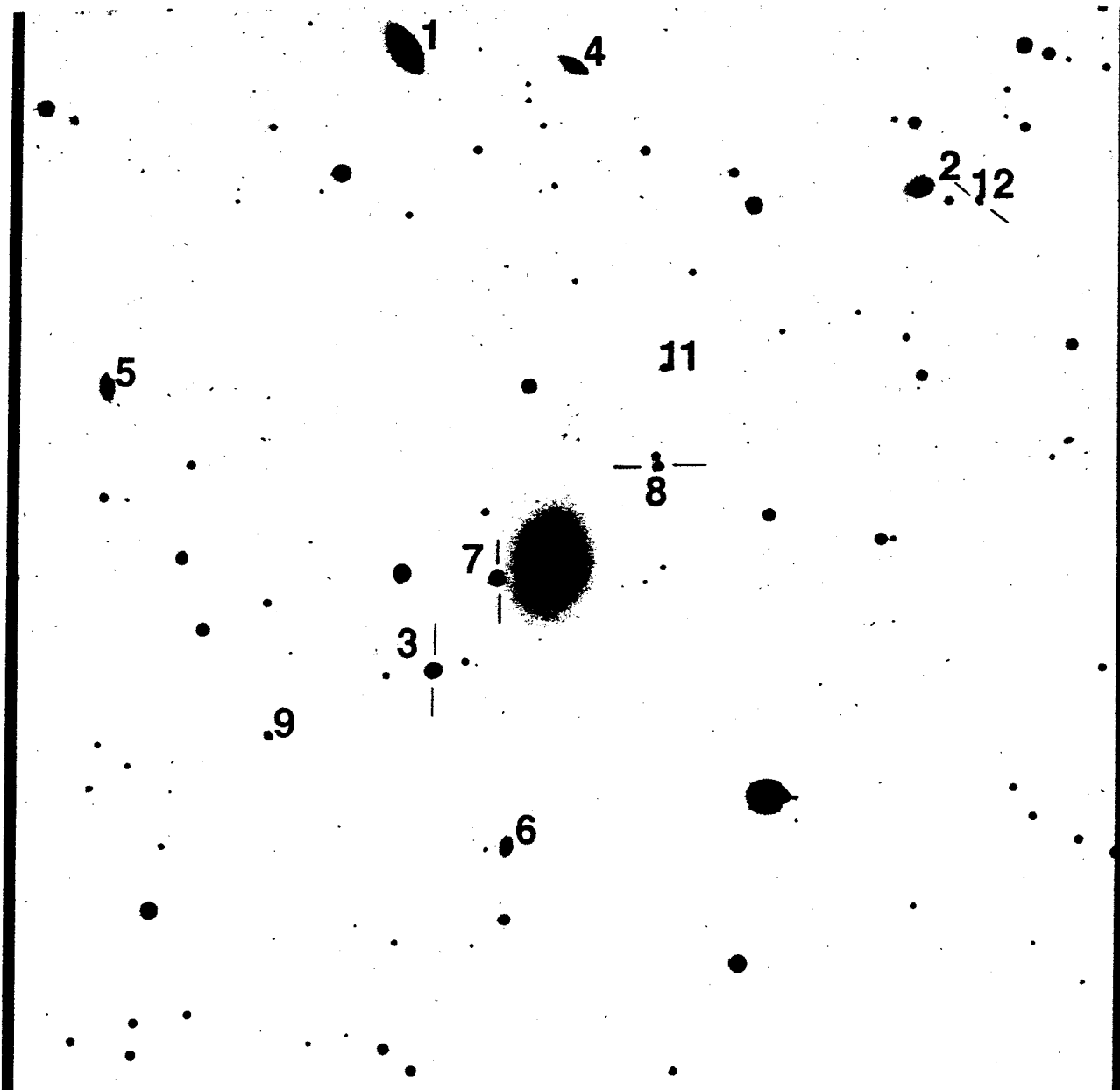| GALAXY NUMBER	$m(R)$	OFFSETS		cz_0 (km s^{-1})	COMMENTS
		R.A.	Decl.		
Mrk 501	13.2	0".0	0".0	10200	
1..................	14.9	56.2	186.7	9980	
2..................	16.1	−133.8	137.2	35520	
3..................	16.3	44.0	−39.1	10090	
4..................	16.6	−6.5	180.8	9730	
5..................	16.8	164.1	63.4	10100	
6..................	17.1	16.3	−102.8	11060	
7..................	17.7	20.8	−5.5	10060	
8..................	18.2	−38.7	35.3	10580	
9..................	18.6	104.1	−62.2	10200	
11	18.8	−40.7	71.8	56700	
12	18.8	−155.0	131.9	35590	
Zw 225.006......	...	...	...	4785	Hα, [O II], Hβ, [O III]

FIG. 7.—Optical field of Mrk 501. This Gunn R-band image is approximately $7'$ square ($\sim 210\ h_{75}^{-1}$ kpc square at the distance of the 7740 km s^{-1} "void absorption" system in this sight line). The numbered galaxies have all been observed spectroscopically, and none are at the redshift of the Lyα absorption systems found along this sight line (see Table 4).

Mrk 501, the Gunn R-band magnitude, and the observed Galactocentric velocity in kilometers per second. A detailed analysis of the optical profile of the host galaxy to Mrk 501 finds no faint companion galaxies closer than galaxy 7 with $B \leq 19$. The faint object just west of Mrk 501 is a star.

All spectroscopic observations were carried out using the Palomar 5 m telescope with the double spectrograph in a long-slit mode observing two or more galaxies simultaneously. Only the data from the blue channel (3800–5000 Å at 10 Å resolution) were used for redshift determinations, as Ca II H and K were included in this wavelength range for all objects observed. Spectra were cross-correlated with standard elliptical galaxy spectra using the routines described in Ellingson & Yee (1994). Errors in recession velocity measurements are estimated to be ± 100 km s^{-1}.

No galaxies were found at the redshift of either the definite or tentative Lyα absorption systems detected in this sight line. Almost all of the galaxies in this field are within the Great Wall and so likely associated physically with Mrk 501 itself. The local galaxy density around Mrk 501 is similar to that found around other low-z BL Lac objects (Wurtz et al. 1995). A few other galaxies are background. Because of the absence of close galaxies at the redshift of the 7740 km s^{-1} void absorber, we find no galaxy with $B \leq -16$ within 100 h_{75}^{-1} kpc of the "void" Lyα cloud. Similarly, there is no galaxy with $B \leq -15$ within 75 h_{75}^{-1} kpc of the lower redshift (4870 km s^{-1}) Lyα cloud, so that the nearest known galaxy to that system remains 510 h_{75}^{-1} kpc away. The corresponding numbers for the tentative Lyα "void" absorption system at 6210 km s^{-1} are $B \leq -15.4$ within 80 h_{75}^{-1} kpc. Because these limits are 2–3 mag less lumi-

nous than the LMC and just brighter than the Local Group dwarfs, we find no evidence that low-luminosity galaxies produce the Lyα forest clouds in this sight line.

However, the image presented in Figure 7 is not sufficiently deep (limiting surface brightness ~23 mag arcsec^{-2}) to reveal low surface brightness galaxies near the Mrk 501 sight line similar to those found by Impey, Bothun & Malin (1988) and Davies (1993) and collaborators; e.g., Malin 1 has a central disk surface brightness of greater than 25 mag arcsec^{-2}. Only for the two 3C 273 Lyα absorptions in the Virgo Cluster can the presence of low surface brightness galaxies be ruled out (M93).

A new optical spectrum of Zw 225.006 (1651.0+3927, the nearest neighbor to system A, the $cz_0 = 4870$ km s^{-1} Lyα system) was also obtained at Palomar using the same spectroscopic setup described above. This galaxy possesses a "starburst"-type spectrum with strong [O III] ≈ Hβ and strong Hα emission as well as Balmer absorption lines at a recession velocity (see Table 4) 50 km s^{-1} less than the CfA redshift catalog value quoted in Table 4. The use of this new velocity in the "retarded Hubble flow" model described above does not alter the estimated cloud-galaxy distance from the value in Table 3.

4.2. A Sensitive Search for H I 21 cm Emission

The velocities of the two definite Lyα absorption features toward Mrk 501 were observed at the wavelengths of the redshifted H I 21 cm line using the Westerbork Synthesis Radio Telescope (WSRT). Observations were made in 1993 December and in 1994 January and February. We made two 12 hr synthesis observations, centered at 4885 km s^{-1} with short spacings of 36 and 54 m, and a single 12 hr synthesis observation, centered at 7740 km s^{-1} with a 36 m short spacing. The total velocity range covered in each case was 1000 km s^{-1} at a resolution of 17 km s^{-1} per channel. The details of these observations will be presented elsewhere (Carilli et al. 1995).

No H I 21 cm emission above 5 times the rms noise was found at any velocity covered within a 0°.5 radius of Mrk 501. For the 7740 km s^{-1} absorber the observational limits (5 σ) obtained at field center, after smoothing to a velocity resolution of 34 km s^{-1} per channel, correspond to $N(H \text{ I}) \leq 3.9 \times 10^{20}$ cm^{-2} and $M(H \text{ I}) \leq 3.2 \times 10^8$ h_{75}^{-1} $M_\odot$. The primary-beam sensitivity pattern is approximately Gaussian, with a FWHM of 30'. Hence the limits degrade by a factor of 2 at 15' radius and by a factor of 10 at 25' radius.

The corresponding 5 σ limits using the same velocity smoothing as above for the 4870 km s^{-1} absorber are $N(H \text{ I}) < 2.7 \times 10^{20}$ cm^{-2} and $M(H \text{ I}) < 9 \times 10^7$ h_{75}^{-2} $M_\odot$. Thus, no evidence was found for a gas-rich galaxy closer to this absorbing cloud than Zw 225.006, and no evidence was found for tidal debris that would link Zw 225.006 with this absorber. No H I 21 cm emission was detected from Zw 225.006 itself. However, this galaxy is located at the 20% sensitivity point of the primary beam; hence the limits are worse by a factor of 5 than at the field center.

These hydrogen mass limits within 500 h_{75}^{-1} kpc of the sight line at both absorber velocities are quite restrictive relative to normal gas-rich galaxies. Virtually all nearby spiral and irregular galaxies observed in redshifted H I have gas masses exceeding 3×10^8 $M_\odot$. Even most (over 75%) S0 galaxies exceed these limits (Roberts & Haynes 1994). Therefore, we find no evidence from the H I radio observations for a gas-rich, low

optical luminosity galaxy related to either of the Lyα absorbers in the Mrk 501 sight line.

The failure to detect an H I 21 cm emitting object in the observed volume of the void is not surprising given similarly empty fields for "random" void regions surveyed in H I by Szomoru et al. (1994). It does suggest that the presence of the Lyα cloud has not raised the H I 21 cm detection rate dramatically over regions of similarly low galaxy density selected "blindly." The result obtained here for a Lyα cloud located in a void is similar to that obtained by van Gorkom et al. (1993) for the two Lyα clouds in the 3C 273 sight line that are within the volume of the Local Supercluster; no H I detection close to the sight line was made there either. More redshifted H I 21 cm observations of local Lyα clouds are required to quantify their effect on H I detection statistics.

Therefore, despite new observations of the Mrk 501 field, current evidence supports the identification of the 7740 km s^{-1} Lyα absorber as an isolated cloud within a large volume of space devoid of galaxies. It appears that at least some Lyα clouds are not associated with galaxies at all.

5. MODELS FOR Lyα CLOUDS

Models of extended, highly ionized galactic disks have been invoked (Maloney 1992; Hoffman et al. 1993) as a possible explanation of the low-redshift Lyα absorbers. Salpeter (1993) has been a proponent of power-law models of extended disks, with total hydrogen column density $N_H(R) \propto R^{-\Gamma}$, recently advocating models with $\Gamma > 2$ (Hoffman et al. 1993) primarily for mass convergence. However, the extrapolation from the known H I structures at radial distances $R = 20$–30 kpc to extents in excess of 100 kpc requires knowledge that is currently lacking.

The gas at large radii in the disks of spiral and irregular galaxies is confined by the gravity of dark matter halos and photoionized by the metagalactic ionizing radiation field. This model has some basis in the observations of sharp edges in the radial H I distribution of disk galaxies (Corbelli, Schneider, & Salpeter 1989; van Gorkom 1993), which have been modeled successfully as extended gaseous disks photoionized by a metagalactic radiation field (Maloney 1990, 1993; Corbelli & Salpeter 1993; Dove & Shull 1994).

The HST FOS data from L94 suggest that high-column Lyα clouds lie within 150–200 h_{75}^{-1} kpc of bright galaxies, whereas in the HST GHRS sample the nearest galaxies lie at distances of 250–7000 h_{75}^{-1} kpc. The observed frequency of low-redshift Lyα absorbers for $N(H \text{ I}) \geq 10^{13}$ cm^{-2} is one every 3500 km s^{-1} (or $dN/dz \approx 86$); this requires that

$$\frac{dN}{dz} = \left(\frac{\pi R_0^2 c}{H_0}\right)\phi_0(1 + z)(1 + \Omega_0 z)^{-1/2} \approx 86 , \quad (1)$$

where ϕ_0 is the comoving density of absorbers, and $R_0 = (100$ pc$)R_{100}$ is their effective radius at contours $N(H \text{ I}) \approx 10^{13}$ cm^{-2}. The observations at $z \ll 1$ therefore require

$$\phi_0 = (0.68 \text{ Mpc}^{-3})R_{100}^{-2} h_{75} , \quad (2)$$

many times the comoving density of standard L^* galaxies, unless the radial extent of their H I halos is much larger than 100 kpc.

With these requirements in mind, we have examined models of gas photoionization in extended disk galaxies. In the case of NGC 3198, the H I edge occurs at $R \approx 30$ kpc and $N(H \text{ I}) \approx (3$–5$) \times 10^{19}$ cm^{-2} (van Gorkom 1993). This struc-

ture is well fitted (Maloney 1993; Dove & Shull 1994) by an extragalactic ionizing flux $\Phi_{ex} = (1-5) \times 10^4$ photons cm^{-2} s^{-1} incident on a gaseous disk with an exponential radial distribution of total hydrogen column density, confined by a dark matter halo consistent with a rotation velocity $V_0 = 150$ km s^{-1}. In the standard models (exponential gaseous disks) used to fit the H I radial distribution, N(H I) can be extrapolated to the level 10^{13} cm^{-2} at $R \approx 100$ kpc. However, there is no physical reason to choose an exponential radial distribution, other than that this simple function does fit the H I distributions over the observed portions of spiral galaxies. To create halos sufficiently large to explain most of the GHRS Lyα sample requires extents approaching 0.5–1.0 Mpc. Thus, we have explored distributions with profiles of total hydrogen column density $N_H(R) \propto R^{-1}$ or R^{-2}, commencing at a point just beyond the edge of current observations, at $R > 30$ kpc.

Figure 8 shows extrapolations of models for NGC 3198 (Dove & Shull 1994) to H I column densities of 10^{13} cm^{-2} for two power-law extensions. The radial distribution of total hydrogen column density was taken to be an exponential $N_H(R) = (2.1 \times 10^{21}$ cm$^{-2})$ exp $(-R/11$ kpc$)$, out to $R = 60$ kpc, then flattening to R^{-1} or R^{-2}. The galactic halo and disk parameters were taken to fit a flat rotation curve with $V_0 = 150$ km s^{-1} and vertical velocity dispersion $\sigma_z = 9$ km s^{-1}, and the extragalactic flux of ionizing radiation was $\Phi_{ex} = 10^4$ cm^{-2} s^{-1} with a spectrum $I_\nu \sim \nu^{-1}$. For this spectrum, $\Phi_{ex} = (4740$ cm^{-2} s$^{-1})I_{-23}$, where I_{-23} is the specific intensity at 1 rydberg in units of 10^{-23} ergs cm^{-2} s^{-1} Hz^{-1} sr^{-1}. Our choice therefore corresponds to $I_{-23} = 2$.

In the power-law models, the 10^{13} cm^{-2} H I contour is reached at distances $R = 200$ and 500 kpc for R^{-2} and R^{-1} profiles of $N_H(R)$, respectively. The asymptotic behavior of $N_{HI}(R)$ in these models is well described by the analytic approximation (Maloney 1992), in which the hydrogen gas is confined to a Gaussian vertical layer of density

$$n_H(R) = n_H(0) \exp\left[-\left(\frac{z^2}{2\sigma_h^2}\right)\right], \quad (3)$$

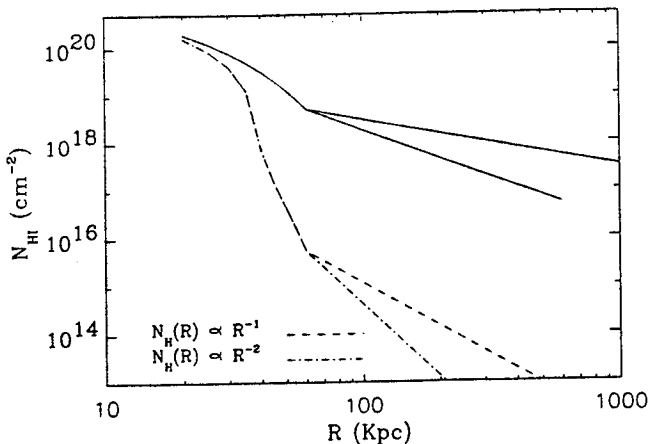whose scale height, $\sigma_h(R) \approx R(\sigma_z/V_0)$, is determined by the halo

gravitational potential with rotation velocity $V_0 = (150$ km s$^{-1})V_{150}$ and gas velocity dispersion $\sigma_z = (18.1$ km s$^{-1})T_{4.3}^{1/2}$ at $T = (10^{4.3}$ K$)T_{4.3}$. The total hydrogen density at the midplane of the disk at radius R is extraordinarily small,

$$n_H(0) = (1.07 \times 10^{-5} \text{ cm}^{-3})T_{4.3}^{-1/2}$$
$$\times V_{150}\left[\frac{N_H(R)}{10^{18} \text{ cm}^{-2}}\right]\left(\frac{R}{100 \text{ kpc}}\right)^{-1}, \quad (4)$$

and the gas pressure, $P/k = 2.3n_H T$, may be unrealistically low. In photoionization equilibrium, the hydrogen neutral fraction is given by

$$X_{HI} = (9.64)T_{4.3}^{-0.726}I_{-23}^{-1}n_H(R, z), \quad (5)$$

where, as before, we have assumed a ν^{-1} ionizing spectrum. In this approximation, the integrated H I column density is

$$N_{HI}(R) = (7.3 \times 10^{13} \text{ cm}^{-2})T_{4.3}^{-1.23}$$
$$\times V_{150}I_{-23}^{-1}\left[\frac{N_H(R)}{10^{18} \text{ cm}^{-2}}\right]^2\left(\frac{100 \text{ kpc}}{R}\right). \quad (6)$$

Since the H I column is proportional to $N_H^2(R)/R$, the neutral column falls off as R^{-5} and R^{-3} for models in which $N_H(R)$ drops as R^{-2} and R^{-1}, respectively.

We have great difficulty believing that such radial extents are possible around bright galaxies. First, such models lead to unacceptably large masses around all gas-rich galaxies; for general power-law disks with $N_H(R) \propto R^{-\Gamma}$, the total gas mass diverges when $\Gamma \leq 2$, although only logarithmically if $\Gamma = 2$. The gas distribution must truncate, along with the dark halo. Second, the gas in such extended disks is quite loosely bound and is subject to tidal stripping. Third, the long dynamic times at $R > 100$ kpc, $\sim(3$ Gyr$)R_{100}^{3/2}$ for a $10^{12} M_\odot$ halo, make it unlikely that the gas would have virialized or settled into a disk. Finally, power-law disks with $\Gamma \approx 2$ are unlikely to explain a distribution in H I column density, $\propto N_{HI}^{-\beta}$, where one finds that $\beta = (2\Gamma + 3)/(2\Gamma + 1)$ from the area-weighted distribution within the disks (Maloney 1992). Models with $\Gamma = 1$ could reproduce the observed distribution, $\beta \approx 1.7 \pm 0.1$, for Ly$\alpha$ clouds at higher redshift (Carswell et al. 1991; Rauch et al. 1992), but they diverge in mass, whereas the R^{-2} disks would produce a column density distribution ($\beta = 1.4$) somewhat flatter than observed. Taken together, these difficulties suggest that the model of extended H I disks is an extremely speculative, unlikely explanation for the observed Lyα clouds.

While it is still possible that there exists a population of low surface brightness galaxies (Impey et al. 1988) or "Cheshire Cat" galaxies (Salpeter 1993) which may have escaped direct optical or H I detection, we find it unlikely that they explain all the characteristics of the Lyα absorbers. When a search for nearest galaxy neighbors to Lyα clouds fails to locate a luminous galaxy within a few hundred kiloparsecs, these nearly invisible galaxies can always be invoked, and their presence is not easily ruled out. However, H I observations by van Gorkom et al. (1993) of two Lyα clouds found by Morris et al. (1991) in the Local Supercluster and our observations of the Mrk 501 clouds suggest two things: (1) there is currently no positive evidence to support this hypothesis, and (2), in order to set very restrictive limits on the presence of such "invisible" galaxies, H I limits significantly lower than those obtained in § 4 (which used excellent Westerboork observations) will be required. Only Lyα clouds discovered within the Local Supercluster ($cz < 2500$ km s^{-1}) will allow that possibility using

FIG. 8.—Column density distributions of total hydrogen (N_H in solid curves) and neutral hydrogen (H I in dashed curves) in models of very extended gas disks. The metagalactic ionizing flux is $\Phi_{ex} = 10^4$ photons cm^{-2} s^{-1}, equivalent to a specific intensity $I_0 = 2 \times 10^{-23}$ ergs cm^{-2} s^{-1} Hz^{-1} sr^{-1} at 1 rydberg for a ν^{-1} spectrum. The distribution of N_H is assumed to be an exponential out to 60 kpc, breaking to R^{-1} or R^{-2} power laws as labeled. The parameters of the galactic potential that confines the gas are for NGC 3198 (Dove & Shull 1994).

even our most sensitive radio telescopes (VLA and Westerbork). The Local Supercluster Lyα clouds discovered in the Mrk 335 and I Zw 1 sight lines will be observed soon in the redshifted H I 21 cm line with the VLA. More examples of such systems need to be discovered by new *HST*/GHRS observations of very bright AGNs to investigate the Cheshire Cat hypothesis further.

Still viable as a possible explanation of the extended associations of H I with galaxies are debris clouds produced by tidal encounters of galaxies. Even at impact parameters ≤ 100 kpc, tidal encounters can significantly increase the area of sky covered by warm or cold H I clouds (Morris & van den Bergh 1994). VLA H I emission maps of low-z metal-bearing quasar absorption-line systems (Carilli, van Gorkom, & Stocke 1989; Carilli & van Gorkom 1992; Womble 1992) have found evidence for disturbed H I in most cases, suggesting that tidal encounters may be important in distributing the gas clouds detected in absorption against background sources; see the H I map of the 3C 232/NGC 3067 system in Carilli & van Gorkom (1992). Unlike the extended galaxy halo model, debris from tidal encounters has the advantage that an unacceptably large mass of gas is not required to create large cloud-galaxy distances. We believe that a tidal origin for some Lyα forest lines requires both a few excellent examples of unambiguous association of tidally stripped gas with an individual Lyα cloud and a few examples of gas-rich galaxies projected close (less than 250 h_{75}^{-1} kpc) to a sight line where there is no detectable Lyα absorption to low column densities. The latter statistic would give clear evidence for a patchy distribution of clouds as expected in a tidal debris theory. Again, both new VLA and Westerbork H I observations and new *HST*/GHRS spectra are necessary to test this hypothesis.

6. DISCUSSION

We have presented *HST*/GHRS high-resolution ($\sim$ 50 km s^{-1}) spectra of three very bright AGNs (Mrk 335, Mrk 501, and I Zw 1) located behind well-defined voids in the distribution of nearby galaxies. These spectra cover the redshift range for Lyα lines of 1500–10,500 km s^{-1} and have signal-to-noise ratios sufficient to detect minimum equivalent widths at 4 σ of 20–100 mÅ, depending upon the object. Eight definite and two tentative Lyα absorption lines have been detected with equivalent widths ranging from 26 to 240 mÅ.

Of the eight definite Lyα clouds, seven are plausibly associated with supercluster structures in the nearby galaxy distribution, although none is close enough to an individual galaxy (≥ 450 h_{75}^{-1} kpc) to be unambiguously associated with it. One definite and two tentative Lyα absorption lines lie within galaxy voids and have nearest known neighboring galaxies 5.9, 6.4, and 10.5 h_{75}^{-1} Mpc away. A pencil-beam optical spectroscopic survey and a redshifted H I search for galaxies or gas clouds near the location of the definite "void absorber" failed to find an optical galaxy to $M(B) = -16$ or an H I cloud with $M(H I) > 7 \times 10^8$ h_{75}^{-2} $M_\odot$ within 100 and 500 h_{75}^{-1} kpc, respectively, of the sight line. Based upon this one detection and three other Lyα absorption lines with no observed galaxies within ~ 4 h_{75}^{-1} Mpc found by Morris et al. (1993) in the 3C 273 sight line, we conclude that voids are not entirely empty of baryonic matter.

Because these *HST*/GHRS observations have probed nearly equal path lengths for Lyα clouds through superclusters and voids, if Lyα clouds are randomly distributed with respect to galaxies, the binomial probability of obtaining the

supercluster/void statistics mentioned above is only $\sim 3\%$. So, even though one "void absorber" was discovered, there is some evidence that Lyα clouds statistically avoid the voids. Clearly, GHRS observations of a few more very bright AGNs are required to verify these results. Our current *HST*/GHRS project will reobserve I Zw 1 and obtain a GHRS + G160M spectrum of the BL Lac object Mrk 421 during *HST* cycle 4. Only a dozen other AGNs are sufficiently distant ($cz > 7500$ km s^{-1}) and sufficiently bright ($V < 14$) to observe in this way. These targets should also be observed in the near future with the GHRS + G160M.

To investigate further the relationship between Lyα clouds and galaxies, we have studied the properties of the 27 local Lyα forest clouds discovered thus far with *HST*/GHRS spectra along five sight lines (our three targets plus 3C 273 [Morris et al. 1991]; PKS 2155−304 [Bruhweiler et al. 1993]) whose environs have been searched for neighboring galaxies. Because no Lyα cloud in this sample lies closer than ~ 250 kpc to a known galaxy, we find no strong evidence for the association of any individual cloud with an individual galaxy. Based upon Monte Carlo simulations of random Lyα cloud placement within the volume of the CfA galaxy survey, we find that (1) Lyα clouds do not cluster as strongly with galaxies as galaxies cluster with each other ($> 99.99\%$ confidence level), but (2) the local Lyα clouds are more correlated with galaxy locations than a random cloud placement would be ($> 99.7\%$ confidence level). Therefore, we confirm the results of Morris et al. (1993), who reached a similar conclusion based upon the 3C 273 absorption systems.

Our results for Lyα absorptions at $W_\lambda < 250$ mÅ are in startling contrast to those found by Lanzetta et al. (1994) based upon much higher equivalent width (> 400 mÅ) Lyα lines found in FOS spectra obtained by the Quasar Absorption Line Key Project team (Bahcall et al. 1993). These investigators always found a bright ($M \leq -19$) galaxy within ~ 100 h_{75}^{-1} kpc of a Lyα cloud and also found a tight correlation between equivalent width and impact parameter, strongly suggesting a galactic halo or extended disk origin for these absorptions (Bahcall & Spitzer 1969; Maloney 1992; Mo 1994). While the 27 local Lyα forest lines in the GHRS sample appear to extend this correlation for another 1.5 orders of magnitude in both variables, a similar correlation is not present in the GHRS data alone. Perhaps, as at high z, there are two populations of clouds: the higher column density, metal-bearing clouds, which are plausibly associated with galaxies, and the low column density Lyα forest clouds, which are metal poor and more randomly distributed with respect to galaxies. By evenly dividing the small GHRS local Lyα cloud sample into two parts at equivalent width $W_\lambda = 100$ mÅ, we find that the lower equivalent width clouds are not inconsistent with random placement with respect to galaxies. While this result is highly tentative, owing to the small numbers of clouds in each subsample (15 and 12 in high and low subsamples, respectively), it suggests that a portion of the local Lyα forest may not be associated with galaxies.

However, none of the above models that associate Lyα clouds with normal galaxies in any way (i.e., extended gaseous halos or disks and tidal debris clouds) can easily account for Lyα clouds in voids, with nearest galaxies located ≥ 4 h_{75}^{-1} Mpc away. Attempts to discover low surface brightness galaxies and Cheshire Cat galaxies (Salpeter 1993) within the nearby voids have not been successful, although further searches should be made. The exciting possibility is that these clouds are truly

intergalactic (Shull, Stocke, & Penton 1995b) and represent the low-mass tail of dark matter–confined clouds, which never formed stars (Rees 1986). This model seems to us to offer no direct observational tests that can easily confirm it, and it may be shown to be plausible only by eliminating the other possibilities mentioned above. If, on the basis of the 27 local Lyα clouds in the GHRS sample, we had found the full sample to be consistent with a random distribution in space relative to galaxies, then this hypothesis would have received strong support and further observations of local Lyα lines might have been of lesser importance. On the other hand, if the GHRS Lyα clouds were all found close (e.g., $\leq 250\ h_{75}^{-1}$ kpc) to galaxies and the full sample had possessed a nearest-neighbor distribution similar to the galaxy-galaxy nearest-neighbor distribution, the major question remaining would be to determine the precise relationship between these clouds and their nearest galaxy neighbor. This eventuality would have required significant follow-up optical imaging and spectroscopy and H I imaging of those nearby Lyα clouds already discovered. But this eventuality would not have required discovering many new Lyα clouds either. However, neither of the above two eventualities has come to pass, and the local Lyα forest is proving to be as interesting and elusive as the high-z forest. Clearly, new HST/

GHRS observations similar to those presented here are required to discover a much larger number of these low column density clouds, so that their relationship to galaxies, supercluster structures, and voids can be placed upon a firmer basis.

REFERENCES

Bahcall, J. N., et al. 1993, ApJS, 87, 1
Bahcall, J. N., Jannuzi, B. T., Schneider, D. P., Hartig, G. F., Bohlin, R., & Junkkarinen, V. 1991, ApJ, 377, L5
Bahcall, J. N., & Spitzer, L. 1969, ApJ, 156, L63
Bajtlik, S. 1993, in The Environment and Evolution of Galaxies, ed. J. M. Shull & H. A. Thronson (Dordrecht: Kluwer), 191
Bechtold, J. 1993, in The Environment and Evolution of Galaxies, ed. J. M. Shull & H. A. Thronson (Dordrecht: Kluwer), 559
Bond, J. R., Szalay, A. S., & Silk, J. 1988, ApJ, 324, 627
Brandt, J. C., et al. 1993, AJ, 105, 831
Bruhweiler, F. C., Boggess, A., Norman, D. J., Grady, C. A., Urry, C. M., & Kondo, Y. 1993, ApJ, 409, 199
Carilli, C. L., & van Gorkom. J. H. 1992, ApJ, 399, 373
Carilli, C. L., van Gorkom, J. H., & Stocke, J. T. 1989, Nature, 338, 134
Carilli, C. L., van Gorkom, J. H., Stocke, J. T., Perlman, E. S., & Shull, J. M. 1995, in preparation
Carswell, R. F. 1988, in QSO Absorption Lines, ed. J. C. Blades, D. A. Turnshek, & C. A. Norman (Cambridge: Cambridge Univ. Press), 91
Carswell, R. F., Lanzetta, K. M., Parnell, H. C., & Webb, J. K. 1991, ApJ, 371, 36
Charlton, J. C., Salpeter, E. E., & Hogan, C. J. 1993, ApJ, 402, 493
Corbelli, E., & Salpeter, E. E. 1993, AJ, 419, 104
Corbelli, E., Schneider, S. E., & Salpeter, E. E. 1989, AJ, 97, 390
Davies, J. I. 1993, in The Environment and Evolution of Galaxies, ed. J. M. Shull & H. A. Thronson (Dordrecht: Kluwer), 105
de Lapparent, V., Geller, M. J., & Huchra, J. P. 1986, ApJ, 302, L1
Dey, A., Strauss, M., & Huchra, J. P. 1990, AJ, 99, 463
Dobrzycki, A., & Bechtold, J. 1991, ApJ, 377, L69
Dove, J. B., & Shull, J. M. 1994, ApJ, 423, 196
Edelson, R., Pike, G. F., Saken, J. M., Kinney, A., & Shull, J. M. 1992, ApJS, 83, 1
Ellingson, E., & Yee, H. K. C. 1994, ApJS, 92, 33
Frenk, C. S., White, S. D. M., Efstathiou, G., & Davis, M. 1990, ApJ, 351, 10
Gilliland, R. L., Morris, S. L., Weymann, R. J., Ebbetts, D. C., & Lindler, D. J. 1992, PASP, 104, 367
Hamilton, A. J. H. 1988, ApJ, 331, L59
Haynes, R., & Giovanelli, R. 1989, in Pont. Acad. Sci. Study Week 27, Large-Scale Motions in the Universe, ed. V. Rubin & G. Coyne (Rome: Specola Vaticana), 31
Heiles, C. 1984, ApJS, 55, 585
Hoffman, G. L., Lu, N. Y., Salpeter, E. E., Farhat, B., Lamphier, C., & Roos, T. 1993, AJ, 106, 39
Huchra, J. P. 1993, CfA Redshift Catalog, 1993 Version (obtained through the Astronomical Data Center)
Huchra, J. P., Geller, M. J., de Lapparent, V., & Corwin, H. G. 1990, ApJS, 72, 433
Hulbert, S. J. 1993, in Calibrating Hubble Space Telescope, ed. J. C. Blades & S. J. Osmer (Baltimore: STScI), 243
Hunstead, R. W. 1988, in QSO Absorption Lines, ed. J. C. Blades, D. A. Turnshek, & C. A. Norman (Cambridge: Cambridge Univ. Press), 71

Impey, C. D., Bothun, G. D., & Malin, D. 1988, ApJ, 330, 634
Kirshner, R. P., Oemler, A., Schechter, P. L., & Shectman, S. A. 1981, ApJ, 248, L57
Kulkarni, V., & York, D. G. 1993, in The Evolution of Galaxies and Their Environment, ed. D. Hollenbach, H. Thronson, & J. M. Shull (NASA CP-3190), 141
Lanzetta, K., Bowen, D. V., Tytler, D., & Webb, J. K. 1994, ApJ, 442, 538 (L94)
Maloney, P. 1990, in The Evolution of Galaxies and Their Environment, ed. D. Hollenbach, H. Thronson, & J. M. Shull (NASA CP-3084), 1
———. 1992, ApJ, 398, L89
———. 1993, ApJ, 414, 41
Meiksin, A., & Madau, P. 1992, ApJ, 412, 34
Mo, H. J. 1994, MNRAS, 269, L49
Mo, H. J., & Morris, S. L. 1994, MNRAS, 269, 52
Morris, S. L., & van den Bergh, S. 1994, ApJ, 427, 696
Morris, S. L., Weymann, R. J., Dressler, A., McCarthy, P. J., Smith, B. A., Terrile, R. J., Giovanelli, R., & Irwin, M. 1993, ApJ, 419, 524 (M93)
Morris, S. L., Weymann, R. J., Savage, B., & Gilliland, R. L. 1991, ApJ, 377, L21
Morton, D. C. 1991, ApJS, 77, 119
Ostriker, J. P., & Cowie, L. L. 1981, ApJ, 243, L127
Ostriker, J. P., & Ikeuchi, S. 1983, ApJ, 268, L63
Peebles, P. J. E. 1993, Principles of Physical Cosmology (Princeton: Princeton Univ. Press)
Penton, S., Shull, J. M., & Edelson, R. 1994, unpublished IUE-AGN Database
Rauch, M., Carswell, R. F., Chaffee, F. H., Foltz, C. B., Webb, J. K. Weymann, R. J., Bechtold, J., & Green, R. F. 1992, ApJ, 390, 387
Rauch, M., Carswell, R. F., Webb, J. K., & Weymann, R. J. 1993, MNRAS, 260, 589
Rees, M. J. 1986, MNRAS, 218, 25P
———. 1988, in QSO Absorption Lines, ed. J. C. Blades, D. A. Turnshek, & C. A. Norman (Cambridge: Cambridge Univ. Press), 107
Roberts, M. S., & Haynes, M. P. 1994, ARA&A, 32, 115
Salpeter, E. E. 1993, AJ, 106, 1265
Salzer, J. S., Aldering, G. S., Bothun, G. D., Mazzarella, J. M., & Lonsdale, C. J. 1988, AJ, 96, 1511
Sargent, W. L. W. 1988, in QSO Absorption Lines, ed. J. C. Blades, D. A. Turnshek, & C. A. Norman (Cambridge: Cambridge Univ. Press), 1
Sargent, W. L. W., Young, P. J., Boksenberg, A., & Tytler, D. 1980, ApJS, 42, 41
Shull, J. M., Penton, S., & Stocke, J. T. 1995a, in preparation
Shull, J. M., Stocke, J. T., & Penton, S. 1995b, AJ, submitted
Slezak, E., de Lapparent, V., & Bijaoui, A. 1993, ApJ, 409, 517
Steidel, C. 1993, in The Environment and Evolution of Galaxies, ed. J. M. Shull & H. A. Thronson (Dordrecht: Kluwer), 263
Stickel, M., Fried, J. W., & Kuhr, H. 1993, A&AS, 97, 483
Szomoru, A. 1994, Ph.D. thesis, Univ. Groningen
Szomoru, A., Guhathakurta, P., van Gorkom, J. H., Knapen, J. H., Weinberg, D. H., & Fruchter, A. S. 1994, AJ, 108, 491
Tully, B. 1988, Nearby Galaxies Catalog (Cambridge: Cambridge Univ. Press)
Turok, N., & Spergel, D. 1990, Phys. Rev. Lett., 64, 2736

Tytler, D. A. 1987, ApJ, 321, 69
van Gorkom, J. H. 1993, in The Environment and Evolution of Galaxies, ed.
   J. M. Shull & H. A. Thronson (Dordrecht: Kluwer), 345
van Gorkom, J. H., Bahcall, J. N., Jannuzi, B. T., & Schneider, D. P. 1993, AJ,
   106, 2213
Weinberg, D. H., Szomoru, A., Guhathakurta, P., & van Gorkom, J. H. 1991,
   ApJ, 372, L13
Weistrop, D., et al. 1992, ApJ, 396, L23

Weymann, R. J. 1993, in The Environment and Evolution of Galaxies, ed. J. M.
   Shull & H. A. Thronson (Dordrecht: Kluwer), 213
Weymann, R. J., Rauch, M., Williams, R. E., Morris, S. L., & Heap, S. 1995,
   ApJ, 438, 650
Williger, G. M., & Babul, A. 1992, ApJ, 399, 385
Womble, D. S. 1992, Ph.D. thesis, Univ. California, San Diego
Wurtz, R., Stocke, J. T., & Yee, H. K. C. 1995, in preparation
Yee, H. K. C. 1991, PASP, 103, 396